Methods of Synthesis and Characterization of Nanostructures Bridged By Single Molecules

---

An Undergraduate Honors Thesis
Presented to
The Department of Physics
Stanford University

In Partial Fulfillment
of the Requirements for the Degree
Bachelor of Science in Physics with Departmental Honors

Jeremy L. Hiatt

June 2008

Acknowledgements

I would like to thank Professor Goldhaber-Gordon for agreeing to be my honors advisor, as well as for allowing me to join his group in the first place. I would also like to express my gratitude to Professor Chidsey for reading my thesis and providing numerous pieces of helpful advice along the way. Thanks also to Alex Neuhausen, the graduate student whose project I joined last spring, as well as the rest of the members of the Goldhaber-Gordon and Chidsey groups, who tolerated my presence.

I'd also like to thank Menesha Mannapperuma for her unvarnished critiques and unwavering support, as well as my friends Amos, Colin, Owen, and Mary. Finally, I would like to thank Rick Pam, Elva Carbajal, and the Physics Department as a whole for supporting my research enthusiastically, and of course financially.

Preface

I was invited to join this project in April, 2007 by Alex Neuhausen, a graduate student in the Goldhaber-Gordon group. Alex was my mentor, teaching me various techniques and showing me around the lab. Much of the work documented in this thesis was performed in close collaboration with him. Alex took the lead on most aspects of the project, especially in the area of fabrication. I certainly had some input in those areas beyond performing rote tasks. For example, I helped to develop an image processing protocol that converted pictures taken in an optical microscope to a pattern for the SEM.

I was more involved with the chemistry aspects of the project. Last summer, I spent a fair amount of time working on the resin-based "click" method, trying to get it to work. I experimented with many different solvents, trying to find one that would swell the resin to the point where the nanoparticles could penetrate the resin. When I decided to pursue an honors thesis, I was planning on performing the linking reaction with alternate ligands, like diamines. When it failed to work out after a few attempts, and in a similar manner to the failure of the dithiol, I put that project on hold to help Alex get the dithiol linking to work. I spent a fair amount of time trying various phase transfer schemes, hoping to find a viable way to disperse colloid in organic solvent that didn't involve coating the nanoparticles in a thiol monolayer. In summary, I was more autonomous when I was working on the chemistry side of the project, though I felt like I also contributed a fair share to the fabrication and other aspects of the "physics" side.

Table of Contents

Introduction **1**

Chapter 1: Literature Review **3**
1.0.1 Mechanisms of Electron Transport 4
1.1 Solution-Phase Measurements of Single-Molecule Conductance 6
1.1.1 Probing Self-Assembled Monolayers 7
1.1.2 Mechanical Break Junctions with STM 8
1.2 Solid-State Single-Molecule Devices 10
1.2.1 Solid-State Mechanical Break Junctions 10
1.2.2 Fabrication of Gaps by Electromigration 11
1.2.3 Nanoparticle-based Devices 13
1.3 Multi-molecule Electronic Devices and Applications 15
1.3.1 Sandwiched SAM devices 15

Chapter 2: Direct Approach to Dimer Synthesis **19**
2.1 Introduction 19
2.1.1 Establishing Electrical Contact to Nanoparticles 20
2.1.2 Synthesizing Dimers by Direct Addition of Linker Molecule . . 23
2.2 Characterization of the Dimer Mixes 23
2.3 Tweaking the Recipe 26
2.4 Possible Modes of Failure 28
2.5 Gold Colloid in Organic Solvent: Synthesis vs. Phase Transfer 30
2.6 Alternate Ligands 31

Chapter 3: The "Click" Approach **34**
3.1 Resin Approach: Single-Molecule Functionalization 35
3.2 Functionalization/Characterization of the Nanoparticles with Heterogeneous Monolayers 36
3.3 Clicking the Nanoparticles Together 37

Future Directions **38**
4.1 Will Processing Damage the Molecule? 38
4.1.1 Metallized DNA 39

Appendix A: Experimental Methods **41**

A.1 Gold Colloid in Organic Solvent 41
A.1.1 Synthesis 41
A.1.2 Phase Transfer 41
A.2 Dimer Mixes 42
A.2.1 Preparation 42
A.2.2 Deposition Process 42
A.3 Fabrication of Contacts 43
A.4 The "Click" Process 43
A.4.1 Functionalization of the Nanoparticles 43
A.4.2 Performing the "Click" Reaction 43

References **44**

List of Tables

2.1 Dimer counting data 24

List of Figures

1 An overview of the scheme to contact single molecules through click chemistry. From (1). 2

1.1 The Aviram & Ratner rectifier. From (2). 3
1.2 Predicted I-V and differential conductance traces for the BPD molecule. From (3). 5
1.3 Current-Voltage Characteristics of a Coulomb-Blockaded Device . . . 6
1.4 Schematic of a self-assembled monolayer on gold. From (4). 7
1.5 Mechanical break junctions with STM 9
1.6 Conductance as a function of twist angle 10
1.7 Correlated Raman and Conductance Measurements 13
1.8 Trapping and measuring conductance of dimer structures 14
1.9 Redox of the catenane molecule 16
1.10 A molecular electronic memory array 18

2.1 Comparison of Regularity and Aspect Ratio of Contacting Methods . 19
2.2 Locating Dimers 21
2.3 Contacted Monomers 22
2.4 Structure of biphenyl dithiol 23
2.5 Dimers visible during SEM inspection, highlighted by red circles. . . . 25
2.6 UV-vis spectrum of pH-adjusted colloid 25
2.7 Colors of gold colloid 26
2.8 Apparent Raman enhancement with a dimer 27
2.9 X-ray Structure of a Gold Nanoparticle 29
2.10 Alternate ligands 32

3.1 An overview of the steps in the resin-based “click” synthesis 35
4.2 PMMA Outgassing Issues 39
4.3 Carbon nanotubes contacted by metallized DNA 40

Abstract

Nanostructures made of colloidal gold offer much promise in the field of molecular electronics. One of the most basic examples of these structures is the dimer: a pair of gold nanoparticles connected by a single molecule. Typical linker molecules are functionalized on either end with thiol (-SH) groups, since sulfur has a high affinity for gold surfaces. Recently published work presented conductance measurements of single molecules, obtained by electrostatically trapping dimer structures onto gold electrodes.

In this thesis I present several approaches to the synthesis of these dimer structures by a dithiol linker molecule and discuss advantages and disadvantages of each method. The simplest method is to directly add a dithiol linker molecule to gold colloid in aqueous solution. However, insolubility of a typical linker molecule in pure water necessitates a mixed-solvent environment, which can lead to false dimer formation.

An alternate scheme utilizes the azide-alkyne reaction of "click chemistry", in which an azide-functionalized molecule is joined with an alkyne-terminated molecule by formation of a triazole ring structure. In this approach, the gold nanoparticles are first coated with azide-terminated molecules; then, a diacetylene molecule (alkyne groups on each end) is added to link together the azides. I present preliminary characterization data and discuss the feasibility and possible future applications of this approach.

Introduction

The overarching goal of this project is to establish reliable electrical contact to single molecules, combining aspects of chemical synthesis with sophisticated lithography to incorporate a single molecule into a macroscopic electrical circuit in order to measure its conductance. This work falls into the broad category of "molecular electronics", where molecules take the place of traditional circuit elements in hopes of achieving superior performance, scalability, and efficiency compared to semiconductor-based counterparts.

The technique could have a wide variety of scientific applications in chemistry or physics, and also as a screening technique for moletronics devices. Studying conduction through single molecules could give great insight into the properties of electrons in that molecule. Alternatively, one could "fabricate" a quantum system with novel properties in the form of a molecule and then test it using this technique. This technique could also be used as a screening process to test properties of molecules designed for practical application as memory elements, switches, etc. (1).

The following is a general overview of the scheme. The first step is to attach gold nanoparticles to the ends of a target molecule in order to form a dumbbell-like structure, commonly referred to as a dimer. Alternatively, the gold nanoparticles are functionalized with a precursor to the final molecule, and synthetic chemistry joins two particles together. The dimers are then deposited onto a substrate, and conducting leads are patterned to contact each end. The device can then be probed for conductance. The gold nanoparticles scale the end points of the molecule up to a size that can be targeted with lithography. Gold nanoparticles are well suited for this purpose in several respects. Gold colloid is readily commercially available in a wide size range, and even some of the more exotic permutations are easy to synthesize. Also, the process of binding molecules to gold surfaces has been extensively documented, typically in the context of monolayer formation.

That being said, we have recently begun exploring an alternate scheme involving metallized DNA as a replacement for the nanoparticles. The ends of two DNA

strands bind to the target molecule. These DNA strands are subsequently metallized, converting them effectively into wires that are then contacted with patterned leads. One major problem currently with metallized DNA is that the metal tends to form numerous grains rather than a smooth, solid wire. Nevertheless, it remains an attractive alternative to gold nanoparticles.

We found that our original recipe simply failed to produce dimers joined together by a linker molecule, leading to a thorough investigation of why it wasn't working. In this thesis, I discuss the variations attempted on the basic approach, as well as introduce an alternative strategy for dimer synthesis involving "click" chemistry. "Click" chemistry is an approach to organic synthesis that makes use of a small number of highly reliable reactions to link together chemical subunits (5). In this context, "click" offers both simplicity as well as the means to build up complex structures from a few basic subunits. I will present the current state of our attempts to use "click" to make dimers.

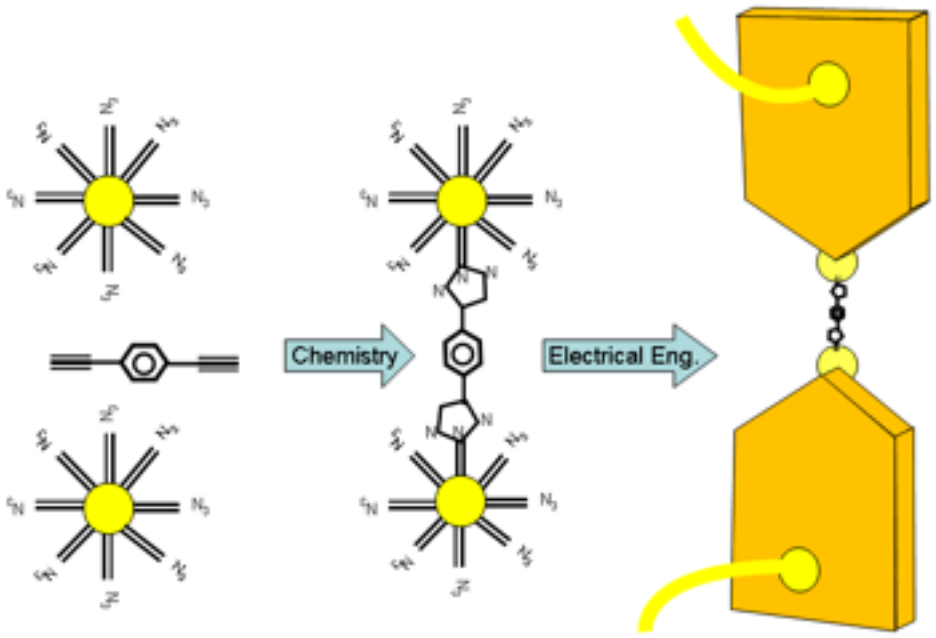

Figure 1: An overview of the scheme to contact single molecules through click chemistry. From (1).

Chapter 1

Literature Review

The field of molecular electronics was born in 1974, when Aviram and Ratner proposed a design for a single-molecule rectifier (2). Their design sought to recreate the familiar p-n junction of semiconductor electronics in the form of two aromatic systems joined together by a methylene group. In this scheme, one of the rings was to be functionalized with electron-withdrawing quino- (=O) groups, while the other was functionalized with methoxy- (-OCH_3) groups.

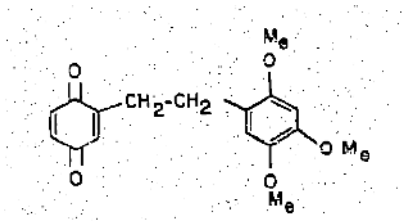

Figure 1.1: The Aviram & Ratner rectifier. From (2).

The molecular orbitals in a conjugated molecule are known as a pi system, referring to the overlapping p-orbitals responsible for double and triple bonding. A phenyl ring is an example of a pi system. When functionalized with substituent electron-donating systems, the energy of the highest-occupied molecular orbital (HOMO) in the pi system is raised, analogously to an n-type, electron-rich semiconductor. If these groups are replaced with electron-withdrawing substituents, then the system becomes electron-poor, and the energy of the lowest unoccupied molecular orbital (LUMO) drops, as in a p-type semiconductor. The Aviram and Ratner rectifier is essentially a p-n junction formed from an electron-poor and an electron-rich pi system separated by a methylene bridge, known as a sigma bridge. The sigma bridge provides a tunneling barrier to prevent strong electronic coupling between the two systems that would result in equilibration of the energy levels across the molecule. The molecule

will theoretically "rectify" because it is much more likely for an electron to go from the electron-rich system to the electron-poor than to travel in the reverse direction.

1.0.1 Mechanisms of Electron Transport

The mechanism for electron transport through a molecule is expected to depend strongly on both the properties of the molecule itself as well as the nature of the contacts (6). Possible schemes for contacting molecules include formation of chemical bonds between the molecule and the electrodes (used in a wide variety of approaches: see following sections) or tunnel junctions across non-bonded contacts (used in solution-phase STM as well as "sandwiched" monolayers). Depending on the properties of the molecule and the contacts, there are several possible phenomena that could occur. Some notable features of the various mechanisms are temperature dependence (or lack thereof, in the case of pure tunneling), behavior at zero bias and low bias, and dependence on gate voltage and applied magnetic field.

Resonant Tunneling One possible mechanism for transport is resonant tunneling through the molecule. In 2003, Xue and Ratner modeled transport through phenyl dithiol (PDT) and biphenyl dithiol (BPD) coupled chemically to metal electrodes through the sulfur atoms (3). At low applied bias, the current is predicted to be roughly linear with voltage, due to tunneling through the HOMO-LUMO gap. They predicted that high applied bias would increase the energy of the HOMO, leading to peaks in the conductance when an energy level lined up with the Fermi level in the metal electrode. These levels are occupied states, corresponding to HOMO, HOMO - 1, etc. See Figure 1.2.

Coulomb Blockade A common phenomenon in low temperature conductance measurements is known a Coulomb blockade, which is manifested as a suppression of differential conductance at zero bias. Coulomb blockade can arise in the simple case of two electrodes separated by a tunnel barrier, or when an island sits between two electrodes. In the case of electronic island states, it occurs when the charging energy required to place another electron on the island exceeds the energy of a conduction electron in the leads. The I-V curve shows characteristic stair step features, with a jump each time another electronic state on the island lines up with the potential energy of a conduction electron (see Figure 1.3). The gap between steps is determined by the capacitance of the island. Another hallmark of Coulomb blockade is that it can be tuned by adjusting a gate voltage. By modifying the electrostatic environ-

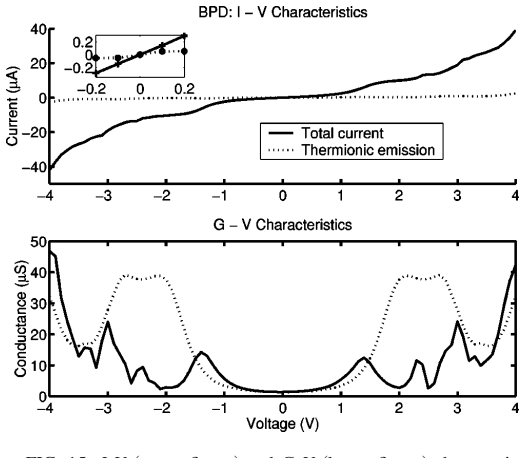

Figure 1.2: Predicted I-V and differential conductance traces for the BPD molecule. From (3).

ment via the gate potential, one can bring the unoccupied electronic states in line with the Fermi energy of the conduction electrons, thereby increasing conductance at zero source-drain bias.

Other phenomena In other devices/molecules, the molecule may act as a pure tunnel barrier, as in the case of "insulating" alkyl chains (6). In these cases, the resistance increases exponentially with distance and is temperature-independent. Alternatively, the conducting electrons can couple to vibrational modes of the molecule, resulting in inelastic scattering (6).

Since the original work in 1974, much effort has been made to establish electrical contact to single molecules. Recent efforts have focused on several main approaches that fall into two broad categories: solution-phase measurements and fabrication of solid-state single-molecule devices. Another class of solid-state devices seeks to exploit the molecular electronic properties of a small collection of contacted molecules. Nearly all of these techniques rely in some way on the gold-sulfur (Au-S) bond as a means of contacting the macroscopic electrical setup to the molecular level, with a few notable exceptions.

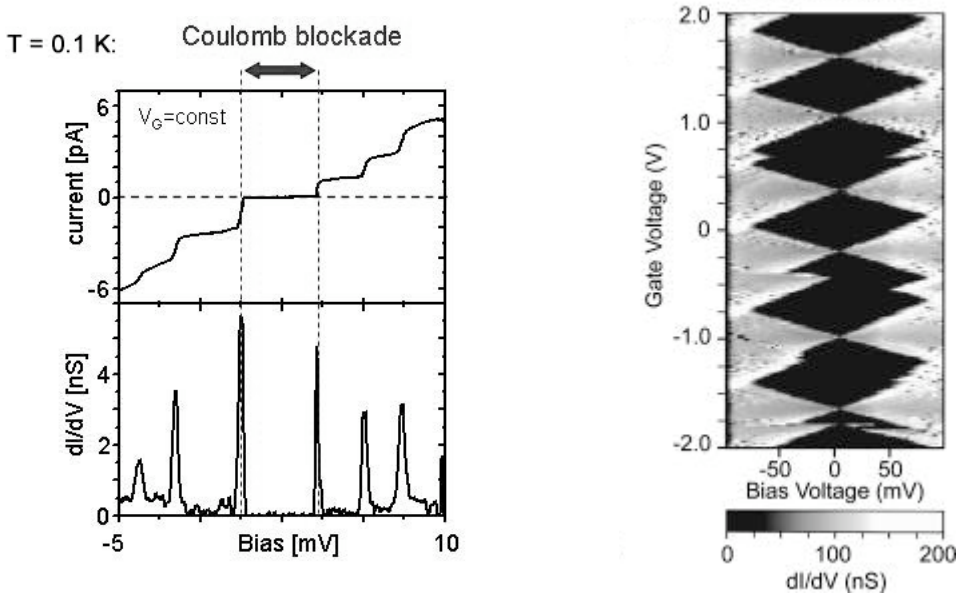

(a) I-V and Differential Conductance Curves at Constant Gate Voltage

(b) Differential Conductance at Varying Source-Drain and Gate Voltages

Figure 1.3: I-V and differential conductance plots indicative of Coulomb blockade. (Left) Note the stair steps in the I-V curve, corresponding to peaks in differential conductance. (Right) The diamond-like features are typical of Coulomb blockade. From (7).

1.1 Solution-Phase Measurements of Single-Molecule Conductance

In a solution-phase measurement, the target molecule is present in bulk solution over a surface, typically gold. In many cases, the measurement requires formation of a self-assembled monolayer (SAM) on the gold surface. One of the most common examples of a SAM, especially in this context, is a monolayer of alkanethiol on a gold surface. See Figure 1.4 for a schematic diagram of a SAM. The favorable binding between the sulfur and the surface gold atoms drives the molecules to form a close-packed monolayer with the alkyl chains pointing out from the surface. A heterogeneous SAM contains more than one type of molecule; in the case of conductance measurements, usually a thiol with conjugated phenyl rings is present in low concentration relative to a diluent alkyl thiol. However, since the hetero-interaction is less favorable than the stacking of alkane chains, the inserted molecule will tend to accumulate at the "grain boundaries" of the SAM, the interfaces of distinct packing domains.

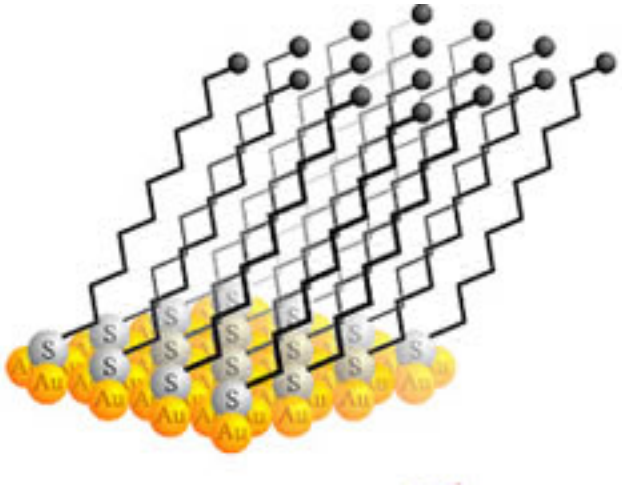

Figure 1.4: Schematic of a self-assembled monolayer on gold. From (4).

1.1.1 Probing Self-Assembled Monolayers

Solution-phase measurements generally make use of high-resolution microscopy techniques to make contact to a singe molecule, or maybe a few molecules. In 1996, Bumm et al. demonstrated the conductivity of conjugated molecules relative to alkyl chains (8). They used a scanning tunneling microscopy (STM) tip to probe a SAM of dodecanethiol that was sparsely populated with a longer conjugated molecule. Though they were able to show qualitatively that the conductance of the conjugated molecules was, as expected, much higher than the conductance of the diluent molecules, they could not make a quantitative assessment of the conductance because of the unknown tunnel barrier between the STM tip and the molecule.

In 2001, Cui et al. reported the use of a similar technique with several key improvements. They formed monolayers of octanethiol interspersed with octanedithiol and then introduced a population of gold nanoparticles. The free thiol groups in the monolayer bound the nanoparticles, which were then located with a gold-coated, conducting atomic force microscopy (AFM) tip (9). By pressing the tip into the nanoparticle, they established electrical contact and constructed current-voltage (I-V) curves for the dithiol. Compared to non-bonded octanethiol molecules, the conductance was four orders of magnitude higher, demonstrating the conductivity of the Au-S bond. However, this type of measurement suffers from complications due to the force required to contact the nanoparticle. In their report, they noted no variability in the measured resistance of a bonded dithiol when varying the applied force. In contrast, when making non-bonded contact the octanethiol monolayer, the authors observed huge disparities in the resistance with varied force, probably due to rearrangement

of the molecules underneath. Also, the nanoparticle frequently contacted multiple dithiol molecules, resulting in steeper I-V curves and lower observed resistance.

1.1.2 Mechanical Break Junctions with STM

An alternative to probing monolayers involves mechanically breaking point contacts between an STM tip and a gold substrate in the presence of molecule. According to the technique originally used to observe quantization of conductance in atomic-size wires, a gold STM tip is driven into a gold surface and slowly retracted. When the contact is stretched, the conductance is reduced in steps of G_0, the fundamental conductance quantum. When only a single gold atom bridges the contact, the conductance is G_0 (11). This technique has been adapted to measure conductance of single molecules by performing the retraction in a solution of the molecule of interest. When a conducting molecule is present, a conductance well below G_0 (usually about two orders of magnitude) is observed after the gold contact breaks. This conductance similarly decreases stepwise, corresponding to a decreasing number of molecules in the junction, until only a single molecule bridges the gap. The process is repeated thousands of times to generate a statistical sample from which the conductance value is extracted. In a 2006 paper, Venkataraman et al. reported that while dithiol molecules made poorly reproducible contact between the surface and STM tip, diamine-functionalized molecules were found to have very well-defined conductance, in the form of strongly peaked samples (see Figure 1.5) (12). They attribute this behavior to the selectivity of the gold-nitrogen bond. They claim that this bond preferentially forms such that the molecule is perpendicular to the surface, the ideal configuration for this type of measurement.

Venkataraman et al. published another paper later that year measuring conductance of substituted biphenyl molecules with distinct twist angles controlled by the side groups on the rings. As expected, they observed a simple cosine-squared relationship between conductance and twist angle (10). One of the major drawbacks of this approach, and of solution-phase measurements in general, is that the measurement cannot be performed at low temperature. It thus seems likely that thermal effects will wash out interesting features. For example, the energy barrier for rotation of a biphenyl molecule is small compared to kT at room temperature. In the paper above, the authors predicted that the molecule would undergo many rotations during the time of a single measurement, so even a single conductance trace for a single molecule represents an average over the ensemble of configurations that the molecule

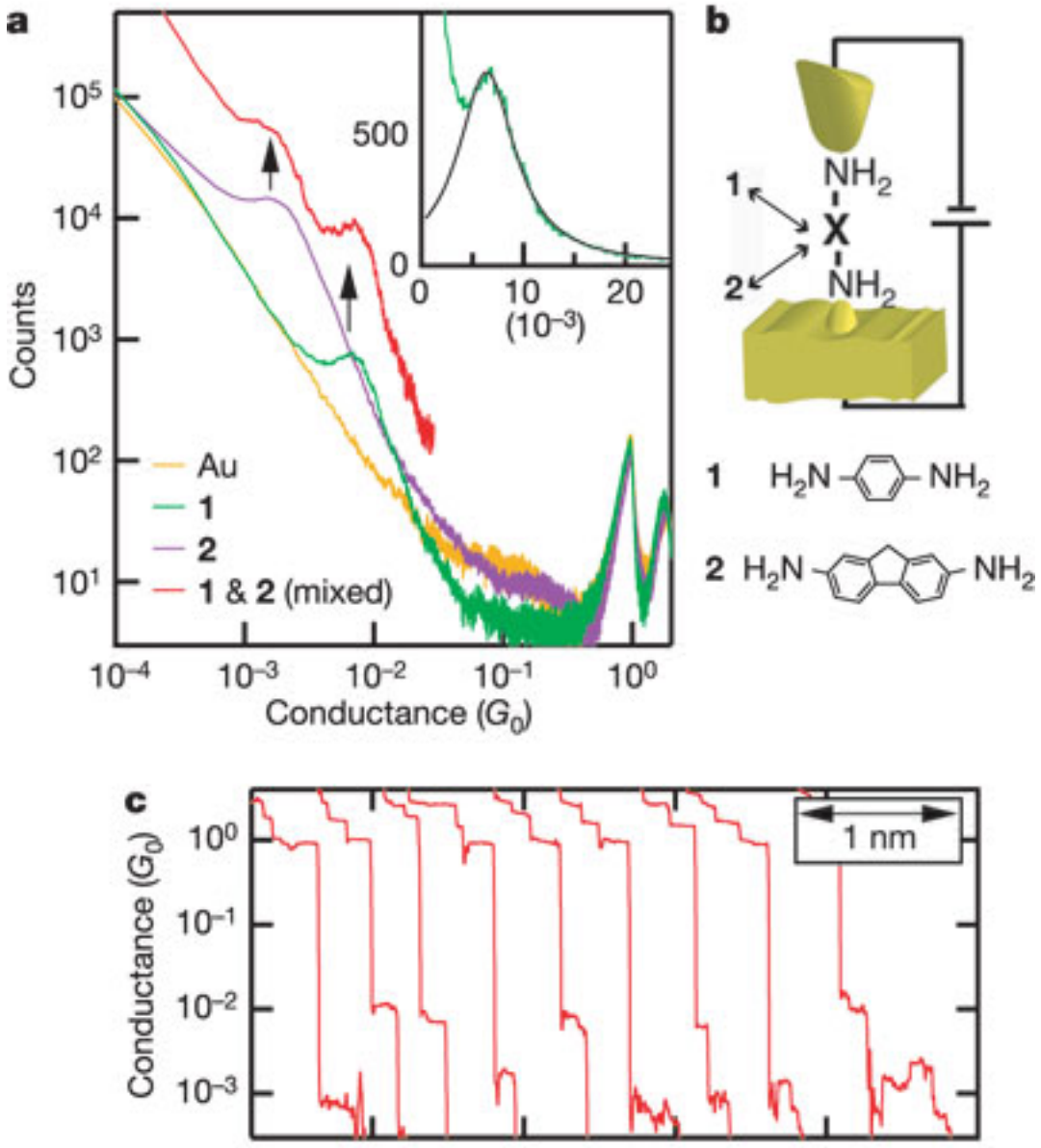

Figure 1.5: **a**, Conductance histograms for molecules **1** and **2** separately, in equimolar concentration, and bare Au, constructed from thousands of measurements on break junctions with STM. **b**, A schematic diagram of a molecule bridging the broken gold contacts. **c**, Sample conductance traces taken when pulling apart point contacts. The steps in conductance are due to molecules **1** and **2**. From (10).

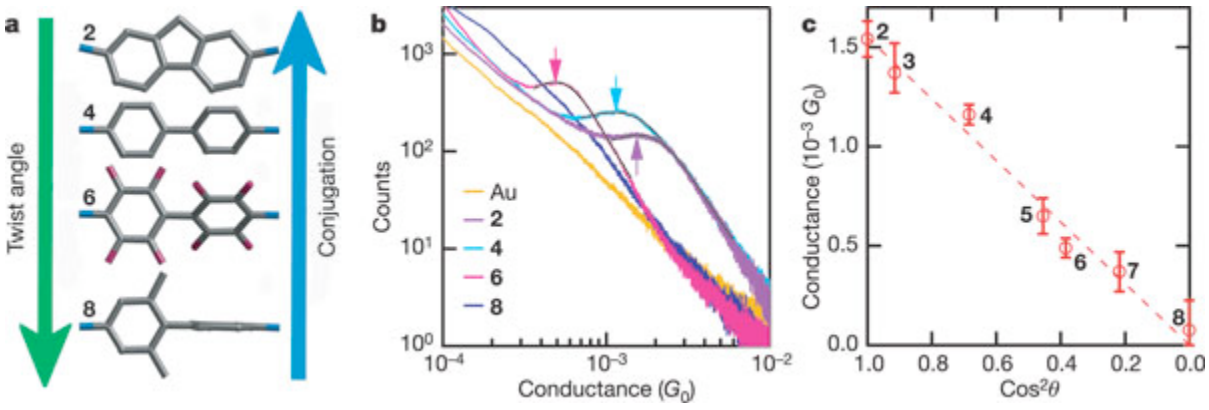

Figure 1.6: (a) Wire-frame models of the molecules used in this experiment, ordered by increasing twist angle and decreasing conductance. (b) Histograms taken from thousands of conductance traces for each molecule, as well as bare gold. Colored arrows indicate inferred conductance value for the corresponding molecule. (c) Plot showing the approximate cosine-squared relation between conductance and twist angle. From (10).

can adopt. This limitation is probably the biggest drawback to solution-phase measurements.

1.2 Solid-State Single-Molecule Devices

A solid-state measurement device is typically manufactured by first fabricating a pair of electrodes separated by a nanometer-sized gap, then depositing a single molecule within the gap to bridge the contacts. In most cases, they can be measured at cryogenic temperatures, though they generally have low yield, and they permit fewer repetitions of a measurement than solution-phase techniques.

1.2.1 Solid-State Mechanical Break Junctions

Several techniques exist for fabricating the narrow gaps needed for a solid-state device. A 1997 paper from Reed et al. reported the use of a mechanically controlled break junction to measure conductance (13). A gold wire was placed on a flexible substrate. Flexing the substrate stretched and broke the wire into sharp points. Varying the applied pressure to the substrate controlled the size of the gap. A solution of benzene-1,4-dithiol was then introduced to form a monolayer on the contacts, and the gap size was reduced until conductance was observed. The authors reported that conductance increased stepwise with bias voltage reminiscent of Coulomb blockade behavior, with

the first step at ∼0.7 V and a corresponding resistance of ∼22 megohms. Occasionally this first feature showed resistance of ∼14 megohms, which they attribute to two molecules conducting in parallel. Since a resistance above 22 megohms was never observed, this was reported to be the resistance of a single molecule. This approach suffers from a few key drawbacks. The authors claim that only a single molecule, or perhaps two, contributes to the conductance of the junction. Instead, a more likely scenario is that one molecule strongly conducts, while many others are weakly conducting in parallel. Also, the devices could not be gated. In recent years, the technique has been refined so that the measurement could be performed at low temperature and even with a gate electrode, though the problem of oddly shaped contacts remains (14).

1.2.2 Fabrication of Gaps by Electromigration

Alternatively, nanometer-sized gaps can be formed by a process known as electromigration. In this process, momentum transfer from conducting electrons to metal ions leads to a concerted motion of these ions in the direction of the current, especially at grain boundaries. Over time this effect can open gaps in a narrow wire. Long known as a common source of failure in integrated circuits, electromigration was applied as a fabrication technique in 1999 to produce nanometer-sized gaps (15). They reported a high variability in the resistance, ranging from hundreds of kilohms to gigohms, of the fabricated tunnel junctions, indicative of variations in the final separation width. The gaps also tended to be non-uniform. Since then, techniques have improved to the point where gaps can reliably be produced with a specific resistance and thus with a specific width. Electromigrated gaps are commonly used as single-molecule contacts because conduction through the gap is believed to take place in a molecule-sized volume, despite an aspect ratio that might seem to support many parallel channels for electron transport. Electromigrated devices can also be probed at cryogenic temperatures. The devices can be back gated by applying a large voltage to the substrate, potentially allowing manipulation of electrical properties of the gap.

These properties of electromigrated gaps have been exploited to explore a number of single-molecule devices. In 2002, Park et al. observed Coulomb blockade as well as Kondo effect in a single-atom transistor: a cobalt ion complex with variable-length insulating tethers spanning an electromigrated gap (16). The characteristic feature of Kondo effect is a peak in differential conductance at zero bias due to coupling between a spin state on the island and the conduction electrons; it is split by an

applied magnetic field and suppressed at finite temperature. When attached with longer tethers the molecule showed Coulomb blockade behavior, and Kondo effect with shorter tethers. The Coulomb blockaded devices could be turned on at zero bias by applying a gate voltage that varied from device to device. Nonblockaded resistance varied by a factor of 10, ranging from ∼100 megohms up to 1 gigohm. This variability was taken as evidence of single-molecule conductance. However, when back gating a device with a given voltage, the electric field felt by the molecule can depend strongly on its environment. In light of the large variation from device to device in the shape of the contacts, it seems problematic to infer single-molecule conductance from variability in this parameter. Yu and Natelson reported similar findings using C_{60} as a single-molecule transistor within an electromigrated gap (17). For a very small number of devices, manipulating the charge state of the molecule with applied gate voltage would result in Kondo-like behavior. One of the major concerns with electromigrated junctions is differentiating between behavior due to the presence of a molecule and the intrinsic properties of the junction. Electromigration frequently leads to formation of metal islands between the electrodes, which can give rise to Coulomb blockade and Kondo behavior (18). Differentiating between conduction through a molecule and tunneling to a metal island can thus be very challenging, and this is one of the weak points of this approach. Another challenge is fabricating the gap so that the minimum separation corresponds to the length of the target molecule. Otherwise, it is easy to imagine how the molecule could bridge a wider area of the gap and conduct in parallel with the small area that dominates tunneling current. While gaps can be precisely fabricated for relatively small resistances, corresponding to small separations, the resistance depends exponentially on separation distance. Thus the technique does not scale well for the larger gaps necessary for longer molecules.

Despite these disadvantages, electromigrated gaps have been used to great effect to demonstrate qualitative behavior of single-molecule conductance. Keane et al. observed hysteretic switching behavior in a three terminal single-molecule device fabricated with electromigration (19). The operation of the device was very weakly coupled to applied gate voltage, registering mild dependence in a few cases. These results suggest the need for a stronger coupling to the molecule than back gating can provide in order to reliably control conduction properties.

Electromigrated gaps have been found to be especially effective as hot spots in surface-enhanced Raman spectroscopy (SERS). A recent paper from Ward et al. reported simultaneous, correlated measurement of conduction and Raman response within an electromigrated break junction (20). Approximately 10% of the time, the

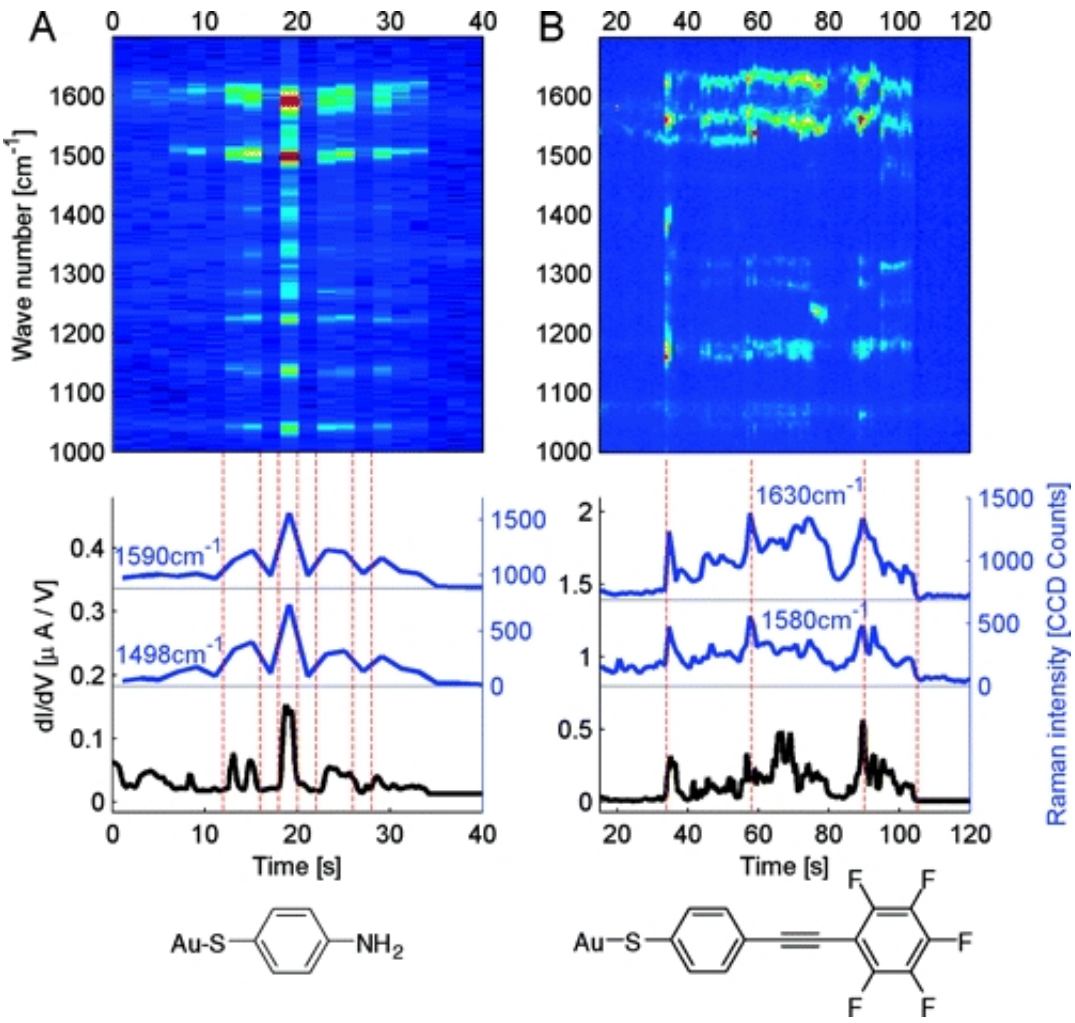

Figure 1.7: Plots showing conductance and Raman intensity correlated in time for two different bridging molecules. From (20).

Raman signal was observed to correlate with changes in the conductance of the junction over time, indicating that the molecule seen in the Raman signal was possibly the same one responsible for conduction. In the majority of devices, however, these signals were uncorrelated, meaning that the Raman enhancement and conduction were spatially distinct and perhaps that the molecule was not involved in conduction at all.

1.2.3 Nanoparticle-based Devices

Solid-state measurement devices can also be achieved without the need for pre-fabricated narrow gaps, offering sharper aspect ratio and better control over the number of molecules in the junction. Gold nanoparticles can be functionalized with

thiol molecules a similar manner to the formation of a SAM on a gold substrate. Long et al. demonstrated a method for assembling molecular junctions using nanoparticles (21). In this scheme, silica nanoparticles were coated with nickel and gold films to render them magnetically susceptible and conducting. The gold surface was then coated with various thiol-functionalized wire molecules expected to show good conductivity. The nanoparticles were then trapped on magnetic pads, and I-V curves were constructed. Though this method cannot be applied to single-molecule measurements, it is an example of a high-throughput, high-yield process to generate molecular junctions.

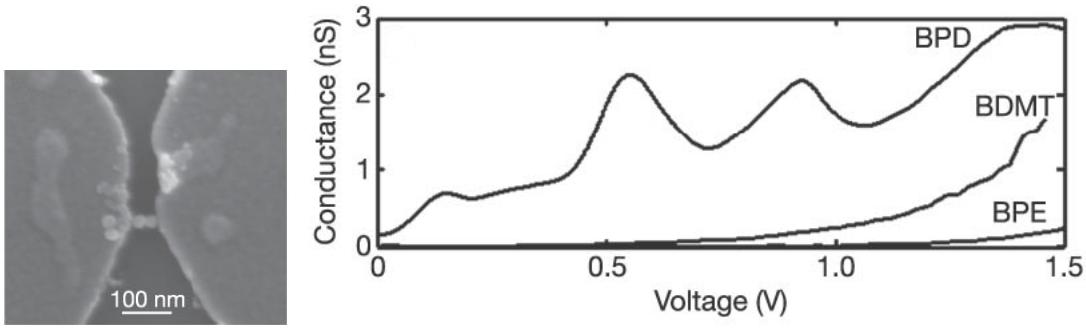

(a) Dimer structure trapped between contacts

(b) Conductance traces for various molecules

Figure 1.8: Trapped dimer approach to single-molecule conductance. (a) A dimer trapped between the contacts. Note the apparent presence of another dimer immediately adjacent. (b) Sample conductance traces for fully-conjugated 4,4'-biphenyl dithiol (BPD), (4-mercaptophenyl)-ether (BPE), and 1,4-benzenedimethanethiol (BDMT). In the latter two molecules, conjugation is broken by additional functional groups. Note the peaks in the BPD trace: these would slide back and forth on the voltage axis in time, but maintain a fixed spacing. From (22).

Most notably, Dadosh et al. reported single-molecule conductance using a nanoparticle-based technique in 2005 (22). In this scheme, the target molecule was introduced to a solution of nanoparticles in extremely low concentration (typically in a 1:10 ratio of molecule to nanoparticle) so that the dimers formed would be bridged by exactly one molecule. The mix was then centrifuged, causing differentiation into bands. Selecting the proper band would yield a concentration of ∼50% dimers as a percentage of total structures. These dimer structures were then electrostatically trapped by applying an ac voltage to a set of gold electrodes, attracting the dimers to the contacts. Once trapped, the sample was dried and cooled to cryogenic temperatures for measurement. As with many of the other techniques discussed here, the yield of working devices was quite low; even then, the results are plagued by high variability

in observed conductance. When measuring conductance of biphenyl dithiol (BPD), the highest conductivity molecule measured, the characteristic shape of the differential conductance plot was reproduced across all devices (see Figure 1.2.3). However, the measured conductances varied by approximately an order of magnitude, and the peaks would shift back and forth over time, which the authors attribute to random gating due to changes in electrostatic environment. Finally, the observed conductance for BPD was several orders of magnitude lower than predicted by theory. When contacting a single gold nanoparticle, the junction resistance was typically 10 megohms, likely due to the tunnel barrier formed by the protective citrate layer on the colloid. This flaw adds complexity to the experimental system, since these leads could in principle exhibit similar conduction properties to a single molecule, as with the metal islands in electromigrated gaps. This concern leads to consideration of a larger issue: one cannot devise a proper control experiment against which to compare the experimental results. It is therefore imperative to demonstrate conclusively that a single molecule is present within the gap. In principle, a nanoparticle-based measurement technique offers some advantage over fabricated gaps, chiefly that it can be extended to three, four, or more terminals involving highly nontrivial molecular structures. At the present moment, however, much work remains to be done improving the quality and reproducibility of the contact to dimers that are unambiguously single-molecule.

1.3 Multi-molecule Electronic Devices and Applications

Many other molecular electronics devices have been fabricated that are not single-molecule, but nevertheless derive their operation from molecular properties and offer great promise for future applications in computing. Despite heated debate over the exact mechanism by which some of these devices operate, recent advances have resulted in the fabrication of impressively capable units.

1.3.1 Sandwiched SAM devices

As with the solution-phase approach, these multi-molecule devices often base their operation on a small set of molecules organized in a SAM. In 1997, Zhou et al. observed rectifying behavior in a SAM of organic molecules sandwiched between two electrodes (23). The SAM was assembled in a nanopore patterned into a silicon nitride substrate, with a layer of evaporated gold serving as the base electrode. The organic monolayer

occupied an area of a little less than a thousand square nanometers. They then evaporated titanium metal onto the top of the monolayer, followed by a layer of gold to serve as the top electrode. During this evaporation, extreme care had to be taken to avoid damaging the monolayer. The I-V curves constructed for these devices showed strong rectification; the current at ±1 V differed by about a factor of five hundred. The authors attributed this rectifying behavior to the asymmetry of the monolayer, consisting of biphenyl molecules functionalized with thiol on one end but not the other. Though this sandwiched monolayer device is clearly ill-suited for single-molecule applications, it has been applied with great success to the fabrication of active moletronic components.

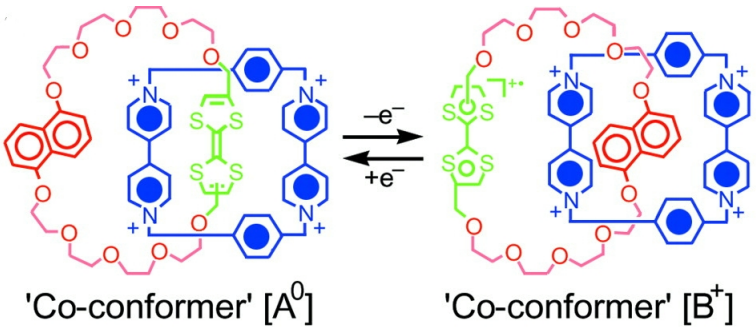

Figure 1.9: Hypothesized structural change of the [2]catenane molecule upon oxidation/reduction. From (24).

In 1999, Collier et al. reported the production molecular logic gates using a type of molecule known as a rotaxane (25). A rotaxane is a dumbbell-shaped molecule with a number of sliding rings trapped in the center: the R(0), R(1) , and R(2) have zero, one, and two crown ether rings, respectively. These three molecules were used in this experiment; each displayed similar behavior. In a similar approach to the one described immediately above, monolayers of rotaxanes were sandwiched between perpendicular metal wires patterned with electron-beam lithography and deposited by evaporation. The active area was at the crossing point of two wires and had an area of a few square microns. By applying a strong oxidizing voltage (+2 V), the molecules were irreversibly switched from on to off and the conductance of the switch, measured at -2 V, dropped by a factor ranging from 50 to 70. Collier et al. published another paper the following year, reporting fabrication of a switch based on catenane molecules (24). By applying voltages of ±2 V, the switch could be thrown open or closed, respectively. Catenanes are composed of interlinking ring structures; the [2]catenane molecule used in this device had two rings. The authors hypothesized that oxidation or reduction of the molecule would cause one of the rings to slide to

a different position on the other ring, thereby changing the conductance (see Figure 1.9). In a key difference from the previous work, the bottom electrode was replaced with n-type polycrystalline silicon (poly-Si) to address concerns that the switching behavior could result from repeated formation and breakage of metallic filaments, given the strength of the electric field (26). A 2004 paper demonstrated that filament formation was the likely primary cause of observed switching behavior in a metal-organic SAM-metal device (27). The use of poly-Si as a bottom electrode should preclude this possibility, but these results nonetheless cast a shadow of doubt on the authors' proposed mechanism of redox-triggered conformational change. Despite the uncertainty, sandwiched SAM devices have been incorporated into impressive computing elements, such as memory arrays.

In 2007, the group responsible for the above work reported the fabrication of a high-density electronic memory unit based on monolayers of [2]rotaxanes (28). At a density of 10^{11} bits/cm^2, the area of a single memory cell was roughly 40 times smaller than that of a conventional DRAM circuit available at the time, demonstrating the scalability that molecular electronics has long promised. However, the yield was low: only $\sim$25% of the memory elements were initially operational. The lifetime was also quite short; most elements would fail after 5-6 cycles, and none lasted longer than 10. This quick failure rate is likely related to the high bias applied to switch the devices, resulting in catastrophically-strong electric fields in the narrow gap. Another major shortcoming of the molecular memory was the speed. A write pulse lasted 0.2s, many orders of magnitude slower than modern DRAM. Still, a moletronics device does not have to be superior to CMOS in all respects in order to be useful. While not likely to completely replace traditional semiconductor devices, molecular electronics devices can potentially complement CMOS devices in the near feature.

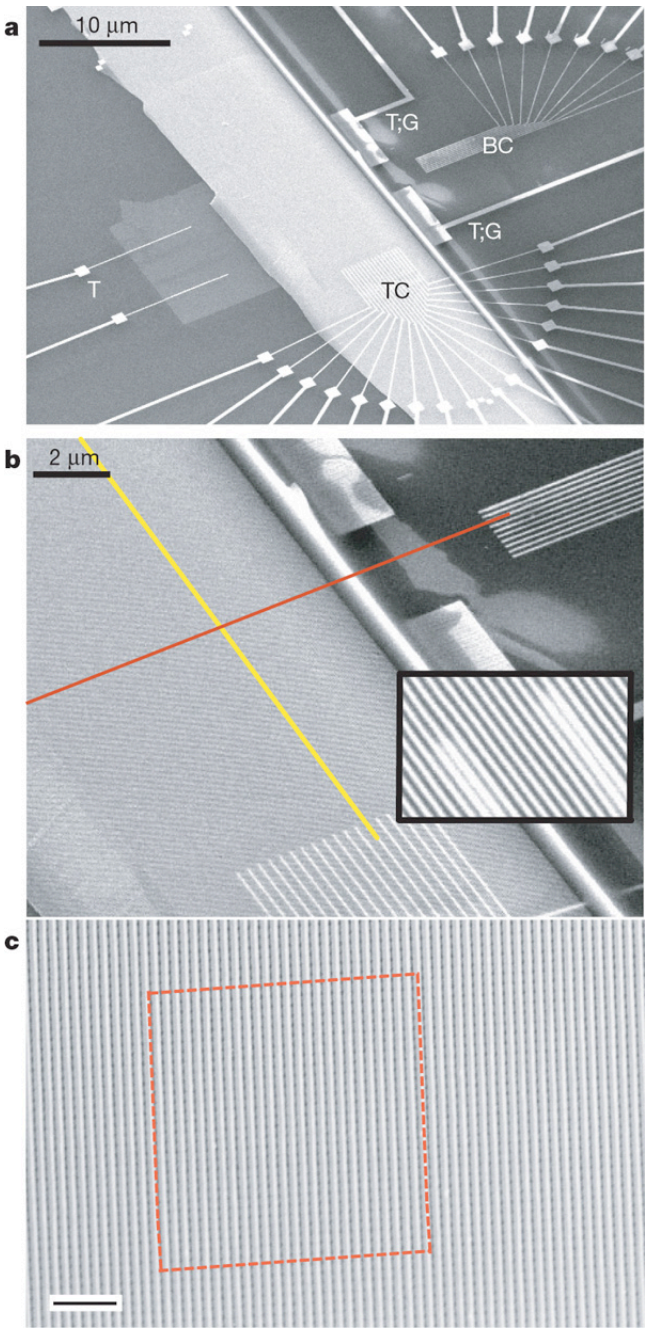

Figure 1.10: A 160-kbit molecular electronic memory array. **(a)** Image of the entire circuit. Each bit is formed by the intersection between one of 400 bottom Si wires and 400 perpendicular top Ti wires. The scale bar is 10 μm. **(b)** An SEM image showing the cross-point of top- (red) and bottom- (yellow) nanowire electrodes. The scale bar is 2 μm. **(c)** High-resolution SEM of approximately 2,500 junctions out of a 160,000-junction nanowire crossbar circuit. The red square highlights an area of the memory that is equivalent to the number of bits that were tested. The scale bar is 200 nm. From (28).

Chapter 2

Direct Approach to Dimer Synthesis

2.1 Introduction

We believe dimer structures synthesized from gold nanoparticles are a promising means of contacting single molecules, despite the challenges we have encountered so far. Gold nanoparticles, as electrical contacts, offer several key advantages over other forms of permanent fabricated contacts (see 1.2). For one, gold nanoparticles (especially those with diameter < 30nm) have a sharp aspect ratio and are quite regular, though the regularity decreases with increasing particle size. Also, the gap width will be determined by the molecule, meaning that the gap can scale up to arbitrarily long distances. For comparison to other methods, see Figure 2.1.

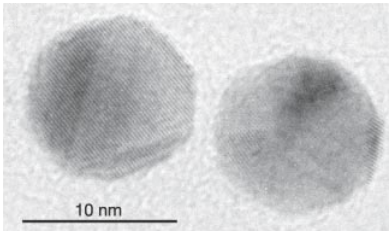

(a) TEM Image of a Dimer (22)

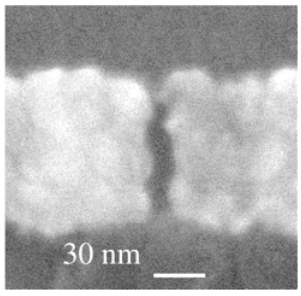

(b) SEM Image of an Electromigrated Gap (17)

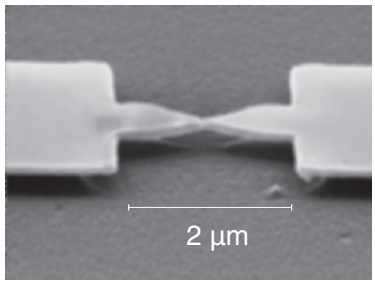

(c) SEM Image of a Mechanically-Controlled Break Junction (14)

Figure 2.1: Comparing various methods of fabricating single-molecule devices. Note the regularity of the nanoparticle surfaces in (a), especially compared to the odd shape of the gap made by electromigration.

2.1.1 Establishing Electrical Contact to Nanoparticles

Though the geometry of a dimer is potentially ideal in the context of binding a single molecule, it has proven challenging to establish a reliable electrical connection between the nanoparticles forming the dimer and the electrodes patterned on a substrate, not to mention the challenges we have encountered in synthesizing the dimers alone. As noted in the previous section, Dadosh et al. pioneered the use of dimer structures as a testbed for single-molecule conductance (see 1.2.3). In these measurements, the dimers were electrostatically trapped between pairs of gold electrodes patterned on a silicon wafer by applying an AC voltage to those pads.

Separation Techniques In order to achieve reasonably high yield of trapped dimers during electrostatic trapping, the dimers must make up a large fraction of the total number of gold structures present in solution. On the other hand, to make dimers bridged by single molecules, the number of linker molecules in the mix is a tenth (or less) of the number of nanoparticles. In a dimer mix, therefore, the concentration of dimers as a percentage of total structures (including monomers and higher oligomers) is capped at about 10%. A couple of separation techniques can, in principle, preferentially separate dimers from monomers based on subtle differences in their properties. Electrophoresis separates particles based on their mobility through a gel under the influence of an electric field. The charge on a dimer[1] should be roughly double that of a monomer, while the drag force on a dimer will only slightly exceed the drag acting on a monomer. Thus, the dimers as a group should migrate more quickly.

Another possible separation technique is centrifugation through a viscous solvent. The centrifugal force acting on a particle scales with mass (which is proportional to r^3, where r is the particle radius), and the drag scales with the cross-sectional area (which is proportional to r^2). Again, the dimers should travel more quickly down the centrifugation tube, owing to the large increase in mass but small increase in cross-sectional area.

Patterning Contacts by Lithography In practice, these separations are quite difficult, and we never achieved much success in concentrating the dimers to an acceptable level for electrostatic trapping despite months of effort with centrifugation

[1] Gold colloid is typically stabilized citrate ions adsorbed to the surface of the nanoparticles. The ions lend an overall negative charge to the particle, causing mutual repulsion between pairs of nanoparticles.

through a glycerol gradient. Very rarely, we would observe the nanoparticles separating into bands. Much more commonly, the nanoparticles would fail to penetrate the glycerol layer at all, and would instead lead down the wall of the sample tube in a dark line. Rather than continue to pursue these challenging separations, we instead developed a novel contacting method, using precision lithography to pattern electrodes directly onto the gold nanoparticles.[2] First, we locate the target structure using a suitable non-destructive imaging technique. Large nanoparticles (diameter $>$ 150nm) are visible in a high-resolution, dark field optical microscope. Smaller particles can be imaged with atomic force microscopy (AFM). Once located, we deposit resist and pattern the leads, connected to larger bond pads, with electron-beam lithography. The leads are deposited by metal evaporation. Following liftoff, the device is placed in a probe station for evaluation, then wire-bonded and cooled to cryogenic temperatures (see appendix for a more detailed description).

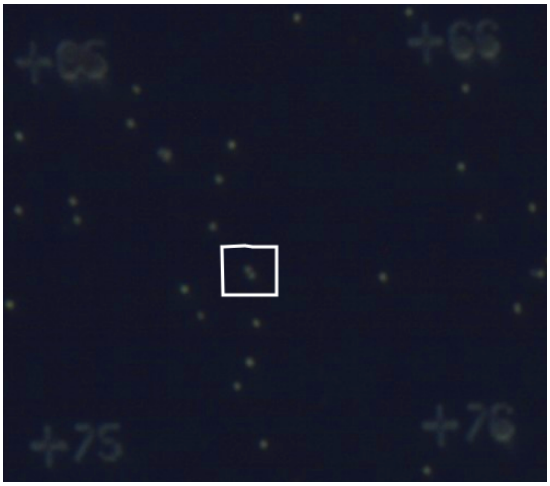

Figure 2.2: An image taken in an optical microscope of 250nm nanoparticles deposited on a silicon surface. A dimer is highlighted by the box. The features in the four corners of the image are alignment markers to facilitate patterning contacts to the dimer.

This approach offers several advantages over electrostatic trapping. First, the quality of contact will be much higher since the metal leads are evaporated directly onto the surface of the nanoparticle. When contacting monomers, the measured resistance was usually between 10 and 30 ohms. At 4 K, the resistance varied from effectively 0 up to roughly 20 ohms. The devices were measured by sourcing a 100nA current at 200 Hz and detecting the voltage across the contacts with a "lock-in" amplifier. The resistance of leads shorted together was measured in a similar manner. This series resistance was subtracted from the measured values for the nanoparticle

[2]Proposed by Joey Sulpizio, who developed a similar technique to contact carbon nanotubes.

contacts to give the reported values. SEM inspection confirmed that the evaporated metal was not shorting out the nanoparticle (see Figure 2.1.1). The metal-metal contact afforded by this method is far superior to the tunnel junction formed during electrostatic trapping, which showed a typical resistance greater by roughly six orders of magnitude. A high-quality contact will suppress phenomena such as Coulomb blockade in the nanoparticles that might otherwise obscure results of single-molecule measurements (see 1.0.1 for an explanation of Coulomb blockade). Second, the relative concentration of dimers is no longer a critical parameter. Especially when using an optical microscope, it is trivial to locate a number of acceptable candidate dimers to contact if their relative concentration on the substrate is 1% or even lower. In Figure 2.2, a dimer is clearly visible in the center of the image. Finally, this technique can be extended to contacting more than two terminals.

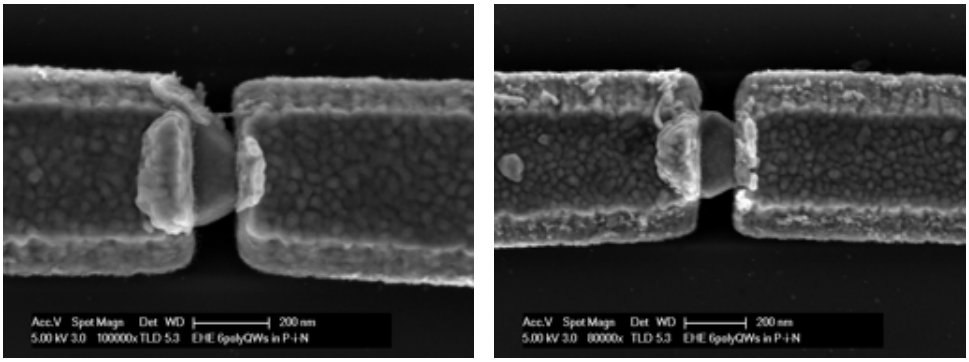

(a) 15 Ω, **5.5** Ω (b) 19 Ω, **10** Ω

(c) 7 Ω, ∼**0** Ω (d) 27 Ω, **16** Ω

Figure 2.3: Various contacted monomers. The resistances reported below each image give the resistance at room temperature and 4 K (bolded). Sourced 100nA current at 200Hz and measured the voltage across the device with a "lock-in" amplifier.

On the other hand, a question still lingers—whether the molecule binding the nanoparticles will survive the processing steps—which we have yet to conclusively resolve. This process will be re-examined and thoroughly tested once we are able to

make dimers that unambiguously contain single molecules. Even if certain steps are found to be problematic, we are reasonably confident that we can find a solution to those issues.

2.1.2 Synthesizing Dimers by Direct Addition of Linker Molecule

Our recipe for dimer synthesis is an adaptation of the method reported by Brousseau et al. in 1999 (29). The following is an example recipe with a final ratio of one linker molecule for every ten nanoparticles. A protected dithiol molecule (4,4'-biphenyl dithioacetate) is dissolved in a mixture of tetrahydrofuran (THF) and ethanol (EtOH) in a 3:2 ratio. The molecule is then serially diluted until the number of molecules in 0.5mL of the final dilution is equal to 1/10th the number of nanoparticles contained 1.5mL of colloid. In a glove bag under nitrogen environment, the diluted molecule is slowly added to the colloid, along with a small amount of ammonium hydroxide (NH_4OH) to cleave the protecting group from the thiol. The mix is allowed to stir for several hours at room temperature before being transferred to a refrigerator.

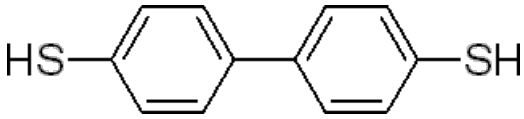

Figure 2.4: Structure of 4,4' biphenyl dithiol, formed by cleaving acetyl groups from protected precursor

We originally believed that the molecule was acting as a linker, based on a positive Raman signal and dimers observed during inspections. However, the Raman results were not reproducible, and the rate of dimer formation was not significantly lower in control samples without the presence of molecule (see Table 2.1). We thus believe that none of the observed dimers was actually joined by a single molecule; instead, the agglomeration was likely due to the addition of organic solvent, which interfered with the mechanism of citrate stabilization.

2.2 Characterization of the Dimer Mixes

The dimer mixes were typically characterized by inspection with scanning electron microscopy (SEM) following deposition onto a substrate. Counting and classifying several hundred objects (monomers, dimers, trimers, etc.) gives an estimate of the relative concentrations of those structures in the bulk sample (see Figure 2.5.) However,

BPD:NP	Mono.	Dimers	Trimers	High Order	% Dimers	Notes
1:20	1613	51	8	3	3%	
1:10	574	25	3	0	4.2%	
1:20	191	31	3	5	13.5%	
Control	217	30	5	1	11.9%	
1:1	600	25	2	4	4.4%	1mM $NaBH_4$
Control	600	24	0	2	3.8%	1mM $NaBH_4$
1:1	600	24	6	4	3.8%	250μM $NaBH_4$
Control	600	23	1	0	3.8%	250μM $NaBH_4$
1:1	600	27	3	1	4.3%	4μM $NaBH_4$
Control	600	36	4	4	5.6%	4μM $NaBH_4$
2:1	126	32	11	23	16.7%	3μM NaOH + O_2
Control	101	27	8	17	17.6%	3μM NaOH + O_2

Table 2.1: Dimer counting data based on SEM inspecting, using 150nm particles. The first column specifies the ratio of linker to nanoparticles; "Control" means no molecule was present. Any alteration of the standard reaction conditions is documented in the "Notes" field.

this technique does not provide direct evidence of the presence of molecule within any of these structures. We have developed the following criteria for inferring the presence of a molecule within the junction. First, a control sample prepared with the same recipe—leaving out the linker molecule—should show few, if any, dimers and higher-order structures. Second, the number of dimers observed should scale linearly with concentration of linker molecule, at least up to some threshold. Dadosh et al. reported that this scaling was evident for ratios smaller than one molecule to ten nanoparticles (22). Satisfaction of the first criteria rules out the possibility that any apparent linking is simply random agglomeration, and in the linear regime, there is a high probability that each dimer is held together by exactly one linker molecule.

A commonly used characterization technique for gold colloid is ultraviolet-visible (UV-vis) spectroscopy, which excites the plasmon resonance responsible for the characteristic color of colloidal gold. The frequency of this resonance is determined by the size of the particles. In a dimer, the surface plasmons on each particle couple together, resulting in small shift relative to the plasmon resonance of a monomer. However, since the shift is quite subtle, the mix must contain predominately dimers in order to observe a difference in the spectrum. When the colloid agglomerates, the plasmon resonance becomes broadens due to the larger size dispersion. See Figure 2.2. Large-scale agglomeration is indicated by a transition to a bluish-purple color.

The dimer mixes were also characterized by Raman spectroscopy. If an apparent dimer actually contains the linker molecule, then it will show a Raman signal due

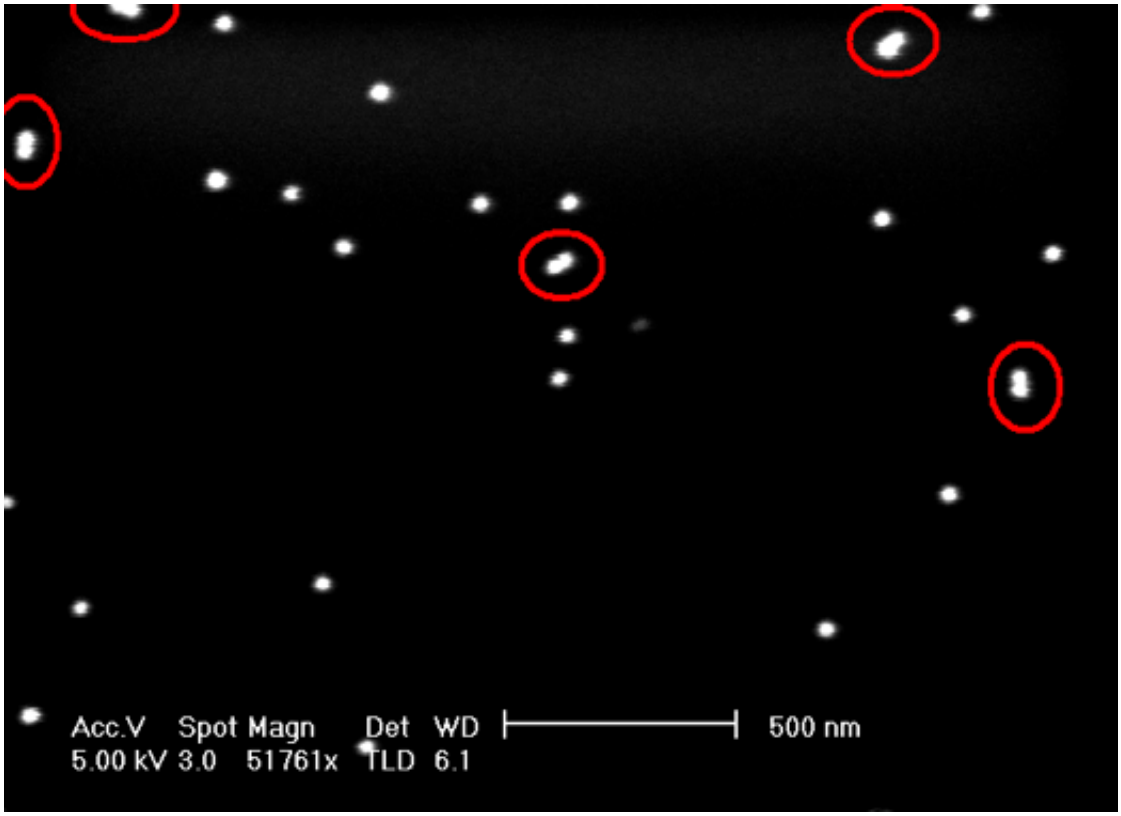

Figure 2.5: Dimers visible during SEM inspection, highlighted by red circles.

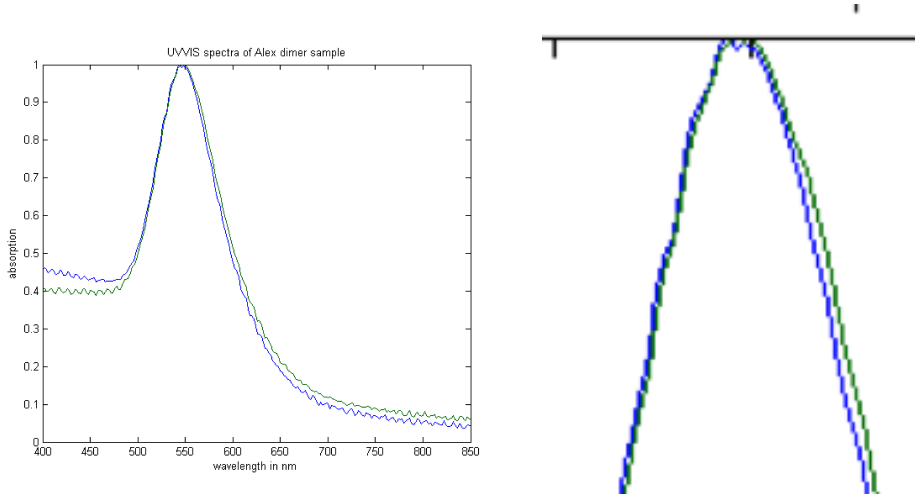

(a) UV-Vis spectrum of pH-adjusted colloid (b) Zoomed in view of the peak

Figure 2.6: UV-vis spectrum of 15nm gold nanoparticles. The blue curve is standard pH, and the green curve shows slight agglomeration due to addition of 1mM acetic acid/sodium acetate buffer.

to the SERS effect. "Blinking", when the signal suddenly drops to zero with no intermediate level, is strong evidence that only a single molecule contributes to the

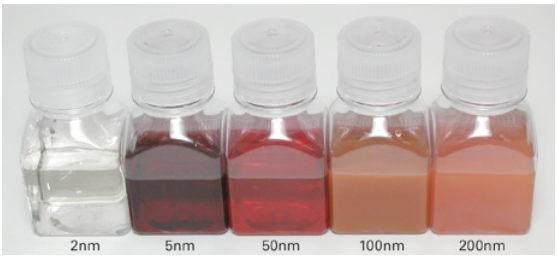

(a) Color of gold colloid determined by particle size. Image from commercial supplier.

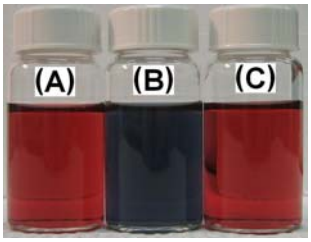

(b) Apparent agglomeration of colloid following acidification, reversed by increasing pH. From (30).

Figure 2.7: Colors of gold colloid. (a) The color transitions from a deep red to a peachy orange for large diameter particles. (b) Agglomeration of 15nm colloid under acidification. Original color shown in **(A)** and recovered in **(C)**. The agglomeration (visible in **(B)**) was reversible in this case due to the presence of a protecting monolayer. See (30). Citrate-stabilized colloid permanently agglomerates under acidic conditions.

observed signal. The signal blinks off when the molecule no longer responds to the incident light, usually as a result of damage to its structure.

On a few occasions, we observed a Raman signal in a dimer mix, seeming to indicate that the dimers were bound by the linker molecule. However, we were unable to replicate these results in numerous repeated efforts. Additionally, we observed no discernible difference between control mixes and varied linker concentrations during SEM inspection. This led us to believe that in fact no linking was taking place. The apparent Raman signal seen on several occasions remains mysterious, but most likely it resulted from some human error, either inadvertent contamination of the sample or addition of the molecule in a concentration several orders of magnitude higher than intended. The latter mistake would actually be fairly easy to make. During serial dilution, if one was to skip the final dilution step, transfer from the wrong solution, or miscalculate the amount to transfer in each step, the final concentration could vary drastically from the expected value.

2.3 Tweaking the Recipe

We came up with several explanations for why the dimer recipe failed to actually produce dimers joined by single molecules. One hypothesis was that disulfide formation between the thiol end groups was polymerizing the linker molecules. Though we were already using a protected thiol, and only performing the deprotection step

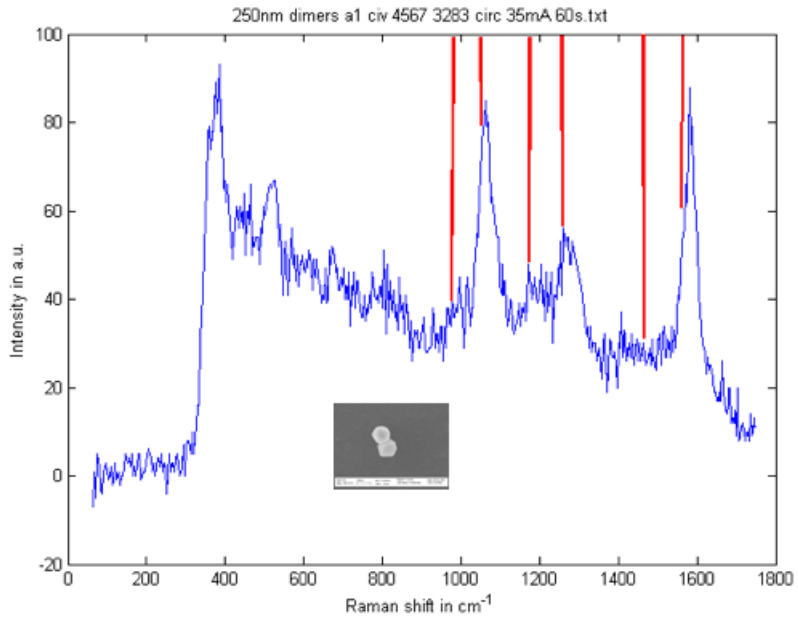

Figure 2.8: Apparent Raman enhancement within a dimer of 250nm nanoparticles. However, results such as these were not reproducible. Inset: SEM image of the dimer supposedly responsible for signal.

in a nitrogen environment, trace amounts of oxygen could have oxidized the thiols to disulfides. To combat the oxidation of the thiols, we added an excess of sodium borohydride ($NaBH_4$), a strong reducing agent. $NaBH_4$ is known to reduce disulfide bonds to free thiols; it is commonly used as a protein denaturant. However, the addition of reducing agent did not result in apparent linking (see Table 2.1).

Another hypothesis was that the formation of the Au-S bond requires the presence of an oxidizing agent, and mixing the reagents under nitrogen was actually inhibiting the linking process. Thus, we stirred the mix in open air and bubbled air through the mix to ensure the presence of oxygen, but we observed no linking (see Table 2.1).

We also considered the possibility that the linker molecule is out-competed by the citrate ions for access to the gold surface. Because it is stabilized by citrate, the conjugate base of a weak acid, the colloid is extremely sensitive to changes in pH. Adding strong acid or base, even in small amounts, will cause rapid agglomeration of the colloid. By making very slight adjustments, one can presumably "dial down" the citrate affinity for the gold surface, opening up small gaps for the linker molecule. Using an acetic acid/sodium acetate buffer, we gently lowered the mix's pH until we observed a discernible difference between a control sample and one with a large excess of linker molecule, as determined by UV-vis spectroscopy. Unfortunately, the control

sample turned out to have ∼5% dimers due to random agglomeration, rendering this method infeasible for the production of single-molecule dimers.

2.4 Possible Modes of Failure

Geometry of the Au-S bond It could be that the problem is one of geometry. Though we idealize the nanoparticles as perfect spheres, in reality their surfaces can be quite irregular, especially at the length scale of a nanometer, the approximate length of the BPD molecule. It could be that the molecule tends not to bind perpendicular to the surface, as would be ideal for linking. In 2007, Jadzinsky et al. published a high-resolution structure of a gold nanoparticle, less than a nanometer in size, functionalized with p-mercaptobenzoic acid (p-MBA). The imaging was done by x-ray crystallography (31) (see Figure 2.9). They observed that the molecule tended to bind to the surface in what they called a "staple motif" involving two sulfur atoms and three gold atoms. These findings have important implications for our work. Namely, the observed oblique binding angle between the p-MBA molecule and the gold surface indicates that our linker molecule may need to be longer in order to effectively stretch between two nanoparticles. Alternatively, we could use a linker molecule with methylene groups on the end to provide flexibility; however, this change would suppress conductance. The observation of the staple motif also suggests cooperativity between pairs of Au-S bonds; perhaps a single Au-S bond is unstable. This hypothesis would explain why monolayers form readily on nanoparticle surfaces, yet single-molecule linking has proved so challenging. The authors also noted stacking of the p-MBA phenyl rings, another point favoring monolayer formation over binding of a single molecule. The evidence noted here suggests a "heterogeneous monolayer" approach might have more success, where a linker molecule is embedded within a monolayer formed by a stub thiol. The diluent thiol could presumably stabilize the Au-S bond of the linker and favorably interact with its hydrophobic phenyl groups. This configuration is essentially the goal of the "click chemistry" approach discussed later (see Chapter 3).

Kinetics The linking may also be significantly hindered by the kinetics of the system. The linking process requires three objects to join together in a specific orientation; each is in very low concentration, and the two nanoparticles are quite massive and thus slow-moving. On the other hand, the assembly can take place in steps, where the linker first binds to one nanoparticle. The linking is then completed when

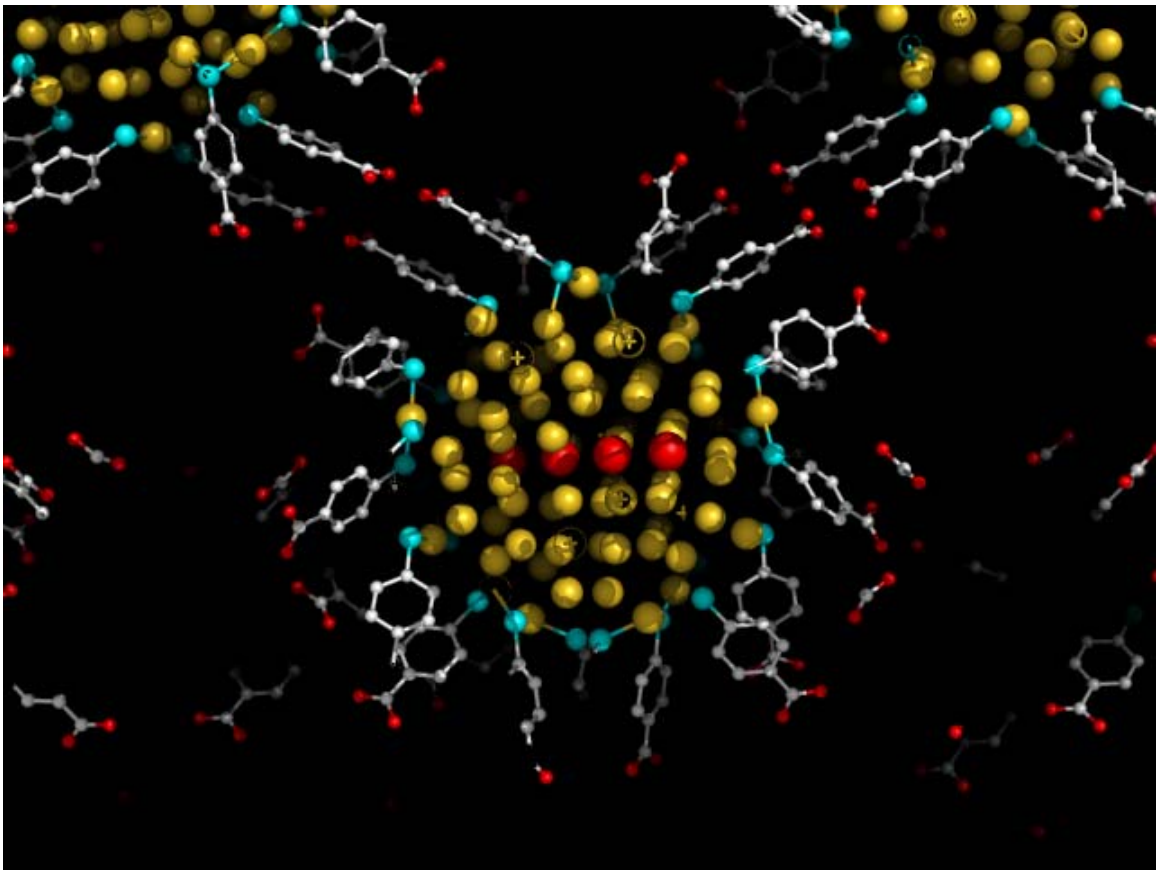

(a) p-MBA Protected Gold Nanoparticle

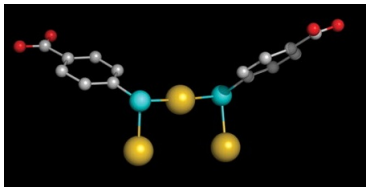

(b) The Staple Motif

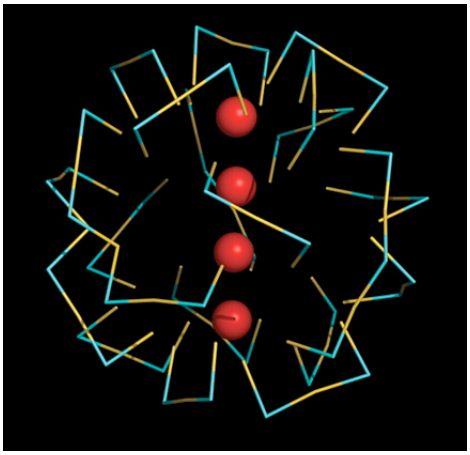

(c) Staples Covering a Nanoparticle

Figure 2.9: Determination of the structure of a p-MBA protected gold nanoparticle by X-ray crystallography. (a) Note the oblique angle made by the p-MBA molecules with respect to the surface. (b) In the staple motif, note the mutual binding of the raised gold atom by the two sulfur atoms. (c) Visualization of the protective layer as a set of staples. From (31).

another nanoparticle comes close enough for the free thiol to bind its surface. Also, the frequency of nanoparticle-nanoparticle collisions must be quite high, given the speed with which the colloid can crash out under adverse conditions. Nevertheless, we tried to address these kinetic issues by allowing the mix to stir longer (24 hrs) at room temperature, as well as maintaining constant stirring after transferring the mix to the refrigerator.

Solvent Environment Another possible issue is the solubility of the linker molecule in the predominately aqueous environment. At such low concentrations, while the molecule may be apparently soluble, it could preferentially partition to the surface phase of the mix, as opposed to the bulk solution phase. Returning again to the citrate stabilizer, it might be that the strongly charged environment of the nanoparticle surface is energetically unfavorable for the molecule. Whatever the exact cause, we investigated the possibility of performing the linking reaction in an all-organic solvent environment more favorable to linker molecule solubility.

2.5 Gold Colloid in Organic Solvent: Synthesis vs. Phase Transfer

Numerous recipes have been reported for the synthesis of gold colloid dispersible in organic solvent, representing variations on a recipe developed by Brust et al. in 1994 (32). In this scheme, the gold ions are transferred from the aqueous phase into the organic phase by means of a phase-transfer catalyst. The reduction and particle nucleation then takes place in the organic phase. Particle growth halts when the passivating molecule, an alkanethiol, can completely cover the surface area of the nanoparticles. It is easy to imagine how one could make dimers by this method, introducing a small amount of dithiol complemented by alkanethiol in much greater concentration, thereby synthesizing both the nanoparticles and the dimers in one fell swoop. However, we found it difficult to synthesize monodisperse, regularly shaped colloid with diameters greater than roughly 40nm or so, while our contacting method is ideally suited to larger nanoparticles (diameter >100nm).

These larger nanoparticles are commercially available and are generally monodisperse and regular. However, the commercial gold colloid is only available in aqueous solvent. We briefly explored phase-transfer methods as an alternative to direct synthesis in organic solvent, hoping to combine the convenience and regularity of

commercial colloid with the potentially favorable properties of the organic environment. Several techniques have been reported in the literature for phase transferring gold nanoparticles into nonpolar organic solvent. One method developed by Lala et al. rendered octadecanethiol molecule water-soluble by forming inclusion complexes with cyclodextrin. The water-soluble thiol was then introduced to the nanoparticles, and during vigorous shaking of a biphasic mixture, the gold colloid migrated to the organic phase (33). We followed their recipe and found some success when using thiols with shorter alkyl chains (up to 8 carbons). One of the major drawbacks of this approach, and similarly with the direct synthesis method, is that the linker molecule now must displace covalently bound thiols, as opposed to weakly adsorbed citrate ions, in order to link two nanoparticles.

We considered replacing the stabilizing layer with alkyl amines to facilitate inclusion of the linker into the SAM on the nanoparticle surface. Given the relatively weak coupling between nitrogen and gold atoms, we believed that the linker dithiol could replace the amines and bind to the nanoparticles. Sastry et al. reported a protocol for the phase transfer of gold nanoparticles into toluene using octadecylamine (ODA) as the transfer agent (34). However, we were unable to replicate their results despite several attempts, using nonylamine and dodecylamine instead of ODA. We attempted a similar protocol using several other agents—benzonitrile, benzyl mercaptan, dodecanethiol, and 4-butylaniline—though none proved effective at phase transferring the colloid.

2.6 Alternate Ligands

In light of the results of Venkataraman et al. (see 1.1.2), and those of Jadzinsky et al. (see 2.4), we explored the use of diamines as an alternative to dithiol linker molecules. Though the gold-nitrogen (Au-N) bond is much weaker than the Au-S bond, it appears to preferentially form such that the molecule sits perpendicular to the surface (12). This property would certainly facilitate linking. Using a similar recipe to the standard approach developed for the dithiol molecule, we attempted to form dimers by addition of o-tolidine, a diamine analogous to BPD except for the presence of two methyl groups. As with the dithiol, however, the control sample was not markedly different from one containing the molecule. Consequently, the further use of diamines was put on hold to focus efforts on other approaches.

Bipyridine molecules could represent another substitute for dithiols. Bipyridine has been used occasionally in mechanical break junction measurements with STM,

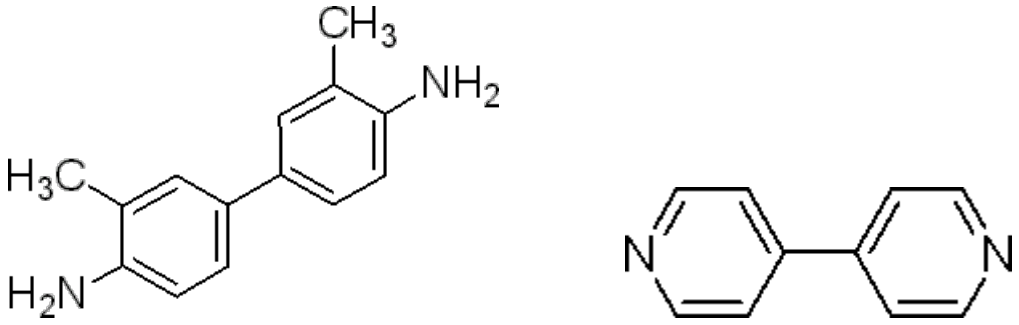

(a) o-tolidine (b) 4,4'-bipyridyl (bipyridine)

Figure 2.10: Alternate ligands

but we were unable to find any reports of SAM formation involving pyridine on a gold surface (35).

Acidification Test We developed a simple test to ascertain the propensity of a given molecule to functionalize the nanoparticle surfaces. Ordinary colloid is unstable under addition of acid, as the citrate ions are protonated and lose their affinity for the gold surface. However, if the colloid is protected by a SAM (an alkanethiol, perhaps) it will remain suspended even after acidification. In the case of pyridine, the results of these tests were puzzling, to say the least. For 15nm colloid, addition of pyridine, even in nanomolar concentration, caused rapid color change and flocculation of the nanoparticles. On the other hand, the 250nm colloid withstood pyridine concentrations many orders of magnitude higher, and it remained suspended following acidification.

An explanation for this disparate behavior could lie in the huge difference in concentration between the two particle sizes. The 15nm colloid is roughly 10,000 times more concentrated (in terms of particles per mL) than the 250nm colloid. Adopting an extremely nave picture of the kinetics of the system (ignoring details such as differences in scattering cross-section and root-mean-square velocities of the nanoparticles owing to their different sizes and masses), we conclude that collisions between the 15nm nanoparticles occur roughly 10,000x more often than between the 250nm particles. Though this factor is almost certainly overestimated, it stands to reason that this difference in timescales could underlie the differing behavior. Perhaps the binding of pyridine molecules to a nanoparticle surface interferes with the citrate coverage, and there is a "critical" time period during which collision with another nanoparticle will result in agglomeration, ending when a monolayer of pyridine has fully formed. Then, we would conclude that for the 250nm particles the protective layer forms

quickly enough that the probability of agglomeration is very low, and not fast enough to prevent agglomeration for the 15nm particles. If this theory is indeed correct, then following sufficient dilution the 15nm colloid should survive the addition of pyridine; likewise, sufficiently concentrated 250nm particles should agglomerate when pyridine is added. However, the factors by which the colloid must be concentrated/diluted to observe these effects are likely quite impractical. Nevertheless, the results with the 250nm colloid suggest that bipyridine may indeed be a viable linker molecule, and it merits further investigation.

Chapter 3

The "Click" Approach

Finally, we sought to make dimers by "click" chemistry rather than direct introduction of a linker molecule. In this approach, the nanoparticles are functionalized with precursors that will be joined together by chemical reaction. The reaction is formally known as Copper(I)-catalyzed Azide-Alkyne Cycloaddition (CuAAC), forming a triazole ring. This reaction is handy for several reasons: it works best in aqueous solvent; it is extremely high-yield; and it works well despite low concentrations of reactants. Joining nanoparticles by this reaction has been previously demonstrated; however, in that work the goal was not to make single-molecule junctions, nor were the molecules particularly interesting candidates for conductance measurements (36). This reaction has also been used to join a molecule to a relatively high-conductance ligand bound to a gold surface, demonstrating its usefulness in the context of electron transport measurements (37).

We have developed the following scheme to make use of the CuAAC reaction. First, the nanoparticles are functionalized with a mix of stub thiols and azide-terminated thiols. When present in suitably low concentration with respect to the stub thiol, each nanoparticle should only have one azide, permitting the formation of dimers but rendering formation of higher-order structures impossible. Following introduction of a diacetylene linker and catalyst, the "click" reaction should proceed to join pairs of nanoparticles. One of the nice features of this reaction is that its yield theoretically could be 100%, unlike dithiol linking which is effectively capped at $\sim$10% if one wishes to stay in the single-molecule regime. Also, with some clever chemistry this method could be applied to make trimers or even more complex structures, though certainly that goal is well beyond our current capabilities.

3.1 Resin Approach: Single-Molecule Functionalization

We originally tried a resin-based synthesis as a means of functionalizing the nanoparticle with a single azide.[1] The nanoparticles were to be passivated with a monolayer capped with diazonium groups. The nanoparticle can then bind to a benzylamine resin. Because of the spacing of the active sites in the resin, the nanoparticle would be bound by exactly one molecule. During the cleave step, this molecule would be converted to an azide, and thus each nanoparticle would be monofunctionalized with azide. See Figure 3.1 below. In practice, however, we found that the nanoparticles were too big to effectively penetrate the pores of the resin. We abandoned the resin-based approach in favor of the less elegant, but hopefully more effective, monolayer method.

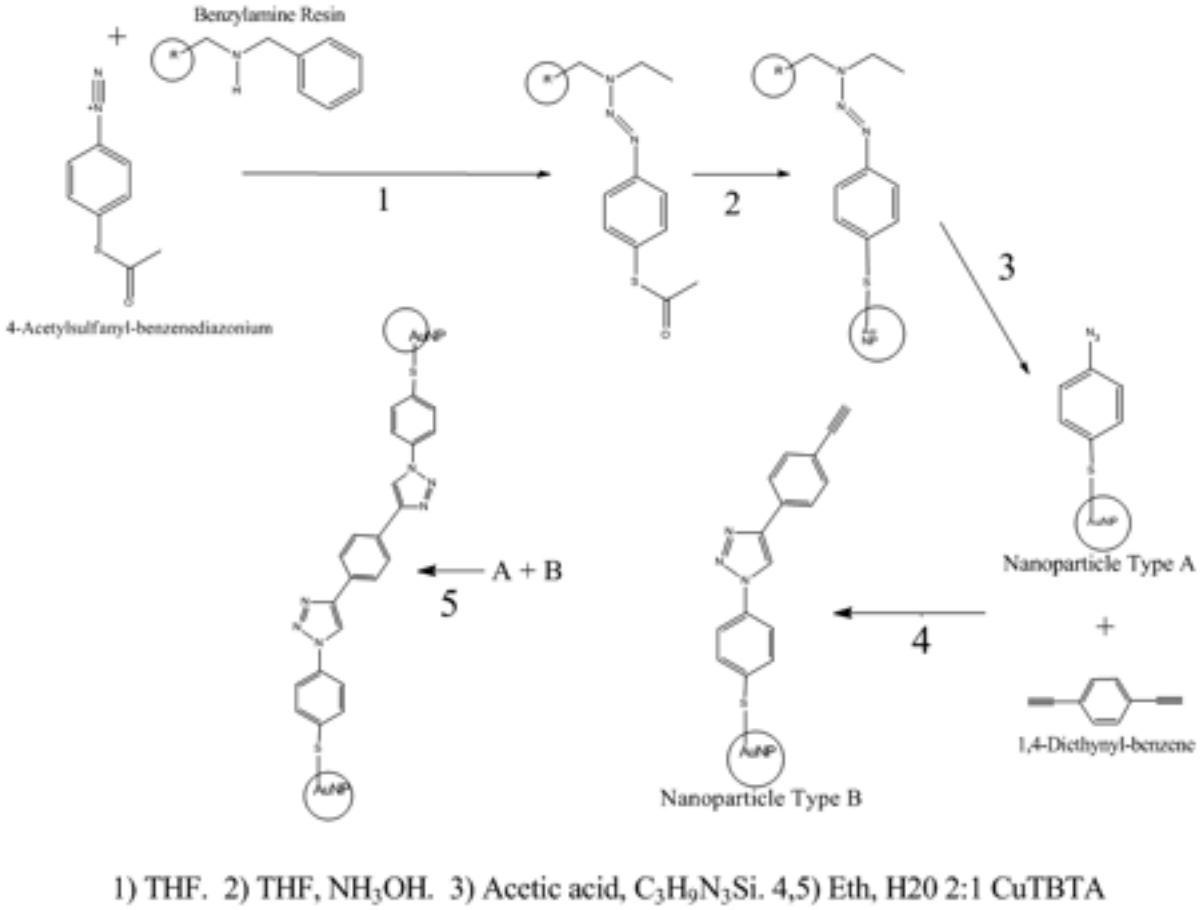

Figure 3.1: An overview of the steps in the resin-based "click" synthesis

[1]Resin-based approach proposed by Wataru Ebina.

3.2 Functionalization/Characterization of the Nanoparticles with Heterogeneous Monolayers

As discussed in earlier sections, the ideal solvent environment for the nanoparticles—pure water—will poorly solubilize organic molecules with long alkyl chains. Here, we report the use of an anionic surfactant to render alkanethiols soluble in the aqueous medium of the gold colloid. Thus, we can functionalize the gold nanoparticles using a minimal amount of organic solvent. We use sodium dodecyl sulfate (SDS) as the surfactant, which is readily water soluble with a critical micelle concentration (CMC) of ∼8mM. As an additional bonus, SDS is also known to effectively stabilize gold colloid. When dissolved in ethanol and introduced slowly, the alkanethiol is incorporated into the micelles formed by the surfactant, thereby providing "reservoirs", so to speak, of thiol to bind the gold surfaces of the nanoparticles.

The nanoparticles can then be characterized by several techniques. First, one can acidify the colloid; if it agglomerates, then it is likely that the monolayer failed to form (see 2.6). The nanoparticles are first centrifuged and re-suspended multiple times in pure water to remove excess thiol and SDS. As a control, we acidified colloid that originally contained only SDS and observed that it agglomerated. The alkanethiol-capped nanoparticles, on the other hand, survived acidification, indicating that a monolayer had indeed coated the gold surface.

Additionally, they can be characterized by X-ray photoelectron spectroscopy (XPS), a spectroscopy method that performs elemental analysis by determining the kinetic energy of electrons ejected from the surface of a sample. Another technique that may prove useful is infrared (IR) spectroscopy, which excites vibrational modes of the bonds between atoms and can be used to identify the presence of certain functional groups.

We are currently working to extend this surfactant-based method to azide-terminated thiols. Initial attempts appear to have failed, based on XPS data as well as the qualitative acidification test. These failures are likely related to the age of the thioazide we were using; perhaps the free thiol has oxidized over time and is now inactive. We have just received a fresh batch and will be retrying this method. The end goal will be to functionalize a nanoparticle with a fully conjugated molecule terminated by thiol and azide groups in order to maximize conductance, with a diluent alkyl thiol to make up the rest of the monolayer.

3.3 Clicking the Nanoparticles Together

Once we have successfully functionalized the nanoparticles with azide, the next step will be to perform the CuAAC reaction to make dimers. The "click" reaction is performed in the presence of copper(I) ions, which serve as a catalyst. Cu^{1+} ions are unstable in aqueous solution, so this catalyst is typically made *in situ* by reduction of copper(II), and stabilized by tris[(1-benzyl-1H-1,2,3-triazol-4-yl)methyl]amine (TBTA). Based on the concern that the reduction of copper ions might plate metal onto the nanoparticles, we add Cu metal, instead of a strong reducing agent, to the reaction mix containing Cu^{2+}. Phenyl diacetylene, a molecule terminated by two alkyne groups, serves as the linker to join two azide-terminated molecules. See appendix for a detailed reaction procedure.

Following the synthesis step, the nanoparticles can be characterized by SEM inspection. IR spectroscopy could also provide evidence of the triazole ring, the product of the click reaction.

Future Directions

Currently, the most promising approach to dimer synthesis appears to be the "click" method, making use of the CuAAC reaction. No doubt, certain aspects of the direct approach deserve to be revisited, such as the investigation of alternate ligands and possible methods of stabilizing the Au-S bond. The CuAAC reaction, on the other hand, has proved to be exceptionally robust, and it has been used to produce structures similar to the single-molecule dimers we hope to make.

Once we can successfully make dimers that unambiguously contain single molecules, we can revisit the contacting technique and hopefully measure electron transport through the bound molecule. In the following section, I have laid out a few of the problems we expect might arise when patterning contacts to the molecule, along with potential solutions.

4.1 Will Processing Damage the Molecule?

One major doubt is that the molecule might become unbound when applying resist. The resist deposition process involves a bake step to remove solvent and harden the plastic. Typical recipes using poly(methyl methacrylate) (PMMA) bake at 180°C for 2 minutes. Such high temperature could potentially cause irreparable harm to the molecule. One concern is the possible dissociation of the Au-S bond. Thermogravimetric analysis (TGA), where the relative weight loss of a nanoparticle is measured with increasing temperature, demonstrates that passivating thiol layers on gold typically begin to vaporize at temperatures ca. 200°C (38). While this is no guarantee that the molecule will emerge unscathed from a bake step at 180°C , it is at least somewhat reassuring. That being said, we can reduce the temperature of this bake step if necessary. The high temperature serves mostly to quickly drive off the solvent. At lower temperatures, baking in a vacuum oven can expedite the solvent evaporation. PMMA undergoes a glass transition around 105°C. We have experienced some difficulties baking below this temperature when depositing a thick layer (>50nm) of

thermally evaporated metal (see Figure 4.2) despite a slow evaporation rate.

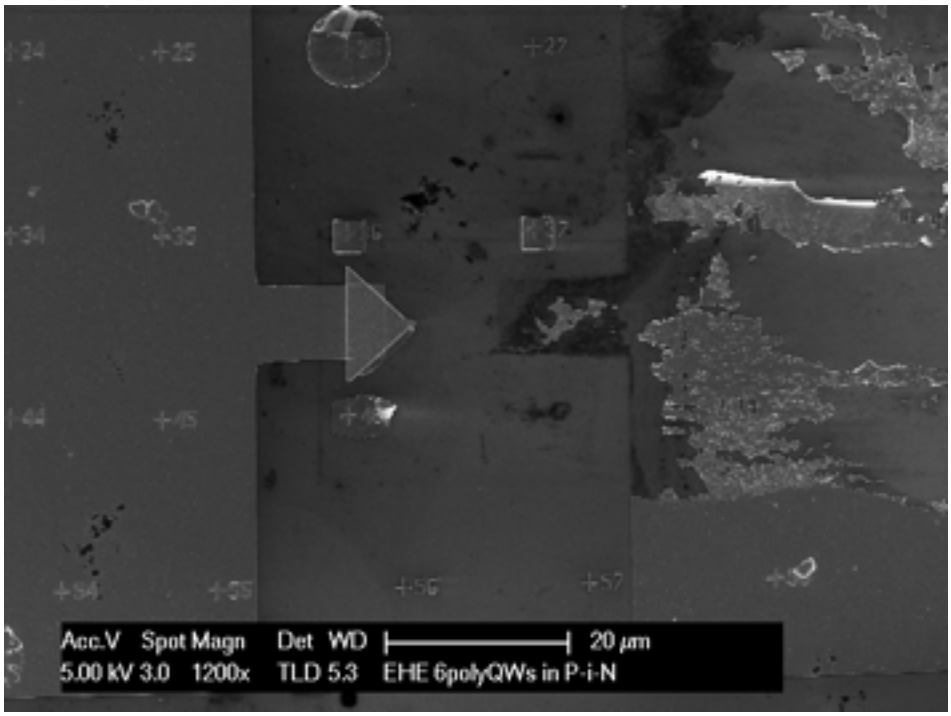

Figure 4.2: SEM image of a device after PMMA outgassed during metal evaporation, possibly due to insufficient baking.

A final concern is if the e-beam lithography itself might damage the molecule, as high-energy electrons are scattered mere tens of nanometers away. Given the molecule's small cross-section, as well as the shield provided by the nanoparticle and thick layer of resist, stray electrons might not pose a threat. However, if this issue arises, it could be addressed by using larger nanoparticles, thereby putting greater distance between the patterned area and the molecule.

4.1.1 Metallized DNA

Another promising area to investigate is the use of metallized DNA to bind to the ends of a molecule. However, many problems remain to be solved before metallized DNA can be used as a reliable electrical contact to single molecules. As noted earlier, grain formation in the metal coating on the DNA results in poorly conducting wires. Probably the biggest question mark is the quality of the contact between the DNA and the target molecule. In 2003, Keren et al. reported the fabrication of a field-effect transistor based on a single-walled carbon nanotube (SWNT) contacted by metallized DNA (39). They noted the presence of a large series resistance in the

device, which they attributed to poor contact between the SWNT and DNA (see Figure 4.3). In order to effectively measure electron transport, the contact between DNA and molecule will need to be well characterized and likely significantly improved.

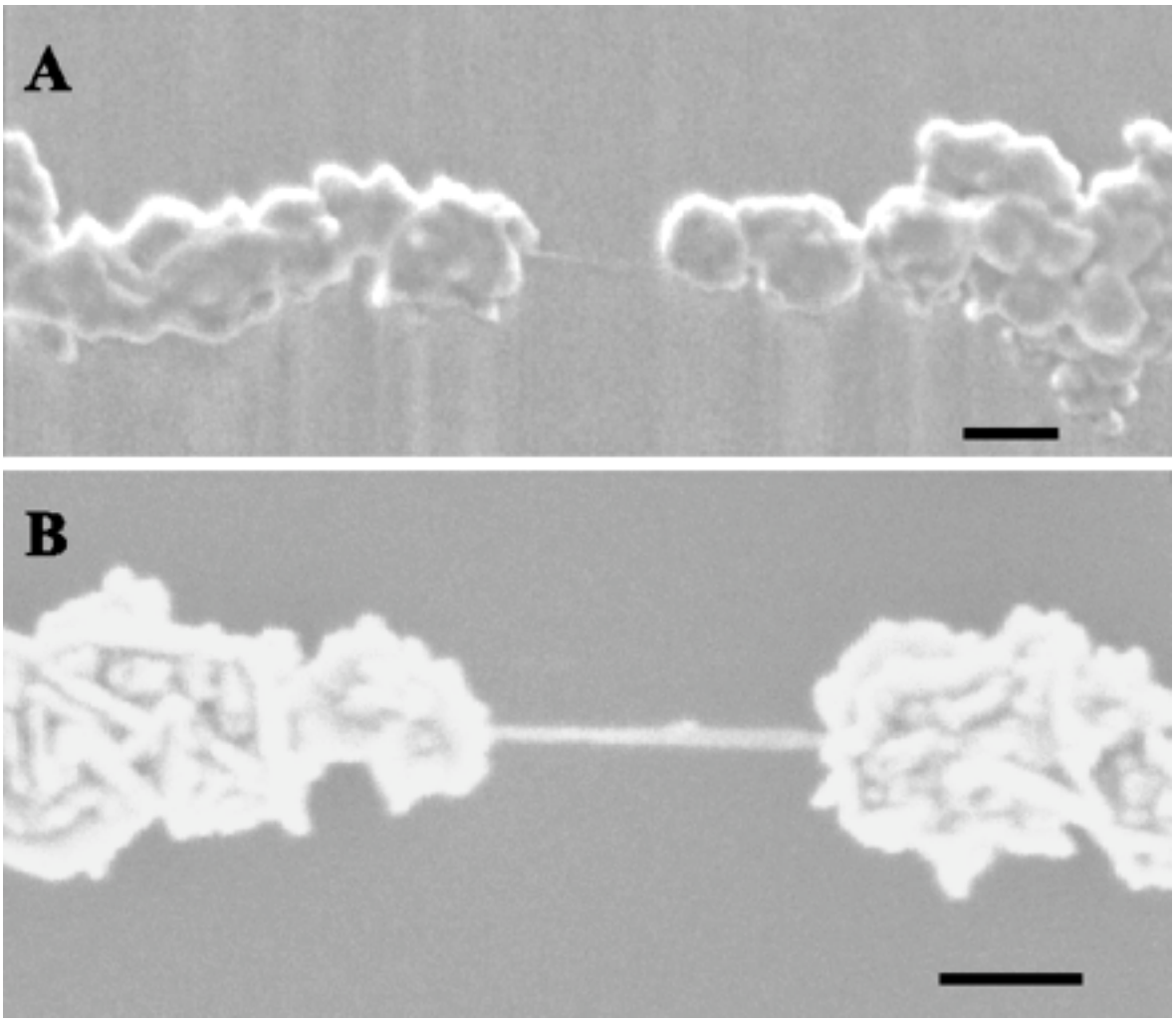

Figure 4.3: Carbon nanotubes contacted by metallized DNA. Note the grains in the "wire." (a) A single SWNT. (b) A rope of SWNTs. Scale bars 100nm. From (39).

Appendix A

Experimental Methods

Chemicals and Glassware All chemicals were used as received from the manufacturer with no additional purification. The gold colloid was purchased from Ted Pella, Inc. Some processes had dedicated glassware; otherwise, disposable 20mL scintillation vials were used for most experiments.

A.1 Gold Colloid in Organic Solvent

A.1.1 Synthesis

Gold colloid in toluene was synthesized following an adaptation of the recipe published by Brust et al. (32). The following is a typical recipe used to make small (diameter ∼5nm) nanoparticles. 17.75 mg of $HAuCl_4$ was dissolved in 6mL of deionized water. 4.0mg of tetraoctylammonium bromide (TOAB) was dissolved in 16mL of toluene. The water and toluene were then mixed, and after stirring for about 20 minutes, the orange color had migrated from the aqueous to the organic phase. 34mg of dodecanethiol was added to the organic phase. Then, a freshly-prepared solution containing 18.9 mg sodium borohydride ($NaBH_4$) in 5mL deionized water was added slowly to the stirring solution. The mix was then allowed to stir overnight. The following day, the organic phase was washed once with dilute H_2SO_4 and twice with pure deionized water.

A.1.2 Phase Transfer

α-cyclodextrin inclusion complexes Following the method of (33), 100mg of α-cyclodextrin was dissolved in 5mL of distilled water and warmed gently to a tem-

perature of 50°C. Then, 1.8μL of octanethiol was added. The mix was allowed to stir for 2 days at 50°C, after which time the octanethiol had apparently dissolved. Then, 1mL of 80nm gold colloid was added, along with 5mL of chloroform. During sonication, the reddish color migrated from the aqueous phase to the organic.

Phase transfer by fatty amines This procedure was adapted from the method reported by Sastry et al. (34). A solution containing 20μL of nonylamine in 1ml toluene was prepared. 1mL of 80nm colloid was then added, but no phase transfer was observed despite vigorous shaking and sonication.

A.2 Dimer Mixes

A.2.1 Preparation

The following is a typical example of a dimer mix, prepared so as to have a 1:10 ratio of linker molecule to nanoparticles. The 250nm colloid contains 3.6×10^{-8} particles/mL. To 1mL of colloid, we added 10μL of NH_4OH to cleave the protecting groups from the linker molecule. The mix was then transferred to a glove bag filled with nitrogen, and we then added 0.5mL of 4,4'-biphenyl dithioacetate (BPDAc) dissolved in 3:2 tetrahydrofuran (THF) / ethanol (EtOH), containing 3.6×10^{-7} molecules of linker. This dilute solution was prepared by dissolving 2mg of BPDAc in 5 mL of 3:2 THF/EtOH, then serially diluting by transferring 40.8μ into another 5mL of THF/EtOH a total of 5 times. The mix was then allowed to stir for about 4 hours before being sealed with parafilm, removed from the glove bag, and stored in the refrigerator at 4°C.

A.2.2 Deposition Process

We deposited gold nanostructures onto silicon (Si) wafers using the following technique. The wafer was placed under an ozone lamp for 10 minutes, then cleaned with acetone, isopropyl alchol (IPA), and Milli-Q water to remove surface contaminants. 25μL of poly-L-lysine was deposited on the surface, and the wafer was spun at 3000rpm to ensure even coverage. This step provides an adhesive layer to bind the nanoparticles. Then, 50μL of the colloid or dimer mix was deposited on the surface and spun at 4000rpm. For the more dilute mixes (i.e. those containing larger nanoparticles), this deposition step was repeated 2-3 times.

A.3 Fabrication of Contacts

An alignment grid with markers spaced by 20μ was patterned onto the Si wafer using standard lithography techniques. Then, the nanoparticles are deposited on the surface as described above. Suitable candidates for contacting are located in an optical microscope under dark field imaging, which makes the nanoparticles very visible. A digital camera attached to the microscope captures an image of the particle and the adjacent grid marks. This image file is then processed to make an alignment file to direct the SEM. The wafer is covered with a thick layer (roughly a micron) of PMMA in multiple deposition steps. Each step is followed by baking in a vacuum oven to remove the solvent. Large bond pads are patterned close to the nanoparticles of interest and 30nm of Ti/Au is deposited. The PMMA deposition is repeated, and the alignment file is used to pattern contacts stretching between the bond pads and the nanoparticles. A thick layer (roughly 200nm) of Au is then deposited by thermal evaporation, since we found that for some reason, electron-beam evaporated gold would not stick to the nanoparticles. During liftoff, the wafer is minimally sonicated to remove excess gold without dislodging the nanoparticles.

A.4 The "Click" Process

The following is a typical procedure for attempting to "click" the nanoparticles. Since there is no diluent thiol, the resulting junction will not be single-molecule.

A.4.1 Functionalization of the Nanoparticles

We prepared 5mL of a 20mM solution of sodium dodecyl sulfate (SDS) in distilled water. To this solution, we added 1mL of 15nm colloid. While rapidly stirring, we then added 50μL of a solution containing 2mg of azido-undecanethiol in 5mL ethanol. Excess azide was then removed by repeatedly centrifuging out the nanoparticles, replacing the supernatant with pure distilled water, and redispersing the nanoparticles.

A.4.2 Performing the "Click" Reaction

The nanoparticles are separated into two populations. To 1mL of nanoparticles, we add an excess of phenyl diacetylene, along with 10μL of 50mM aqueous $Cu(NO_3)_2$, 30mM of TBTA in dimethyl sulfoxide (DMSO), and a small piece of copper metal that has been polished with sandpaper to remove any oxide.

References

[1] A. Neuhausen, Private communication, 2008.

[2] A. Aviram and M. A. Ratner, Chemical Physics Letters **29**, 277 (1974).

[3] Y. Xue and M. A. Ratner, Physical Review B **68** (2003).

[4] Online at: http://www.ehcc.kyoto-u.ac.jp/laboratory/material/material.htm, 2008.

[5] H. C. Kolb, M. G. Finn, and K. B. Sharpless, Angewandte Chemie International Edition **40**, 2004 (2001).

[6] A. Nitzan and M. A. Ratner, Science **300**, 1384 (2003).

[7] K. I. Bolotin, F. Kuemmeth, A. N. Pasupathy, and D. C. Ralph, Applied Physics Letters **84**, 3154 (2004).

[8] L. A. Bumm *et al.*, Science **271**, 1705 (1996).

[9] X. D. Cui *et al.*, Science **294**, 571 (2001).

[10] L. Venkataraman, J. E. Klare, C. Nuckolls, M. S. Hybertsen, and M. L. Steigerwald, Nature **442**, 904 (2006).

[11] N. Agraït, J. G. Rodrigo, and S. Vieira, Physical Review B **47** (1993).

[12] L. Venkataraman *et al.*, Nano Letters **6**, 458 (2006).

[13] M. A. Reed, C. Zhou, C. J. Muller, T. P. Burgin, and J. M. Tour, Science **278**, 252 (1997).

[14] J. van Ruitenbeek, E. Scheer, and H. Weber, Contacting individual molecules using mechanically controllable break junctions, in *Introducing Molecular Electronics*, , Springer Lecture Notes in Physics Vol. 680, pp. 253–274, Springer, 2005.

[15] H. Park, A. K. L. Lim, A. P. Alivisatos, J. Park, and P. L. McEuen, Applied Physics Letters **75**, 301 (1999).

[16] J. Park *et al.*, Nature **417**, 722 (2002).

[17] L. H. Yu and D. Natelson, Nano Letters **4**, 79 (2004).

[18] A. A. Houck, J. Labaziewicz, E. K. Chan, J. A. Folk, and I. L. Chuang, Nano Letters **5**, 1685 (2005).

[19] Z. K. Keane, J. W. Ciszek, J. M. Tour, and D. Natelson, Nano Letters **6**, 1518 (2006).

[20] D. R. Ward *et al.*, Nano Letters **8**, 919 (2008).

[21] D. P. Long *et al.*, Applied Physics Letters **86**, 153105 (2005).

[22] T. Dadosh *et al.*, Nature **436**, 677 (2005).

[23] C. Zhou, M. R. Deshpande, M. A. Reed, L. Jones II, and J. M. Tour, Applied Physics Letters **71**, 611 (1997).

[24] C. P. Collier *et al.*, Science **289**, 1172 (2000).

[25] C. P. Collier *et al.*, Science **285**, 391 (1999).

[26] R. F. Service, Science **302**, 556 (2003).

[27] C. N. Lau, D. R. Stewart, R. S. Williams, and M. Bockrath, Nano Letters **4**, 569 (2004).

[28] J. E. Green *et al.*, Nature **445**, 414 (2007).

[29] L. C. Brousseau, III, J. P. Novak, S. M. Marinakos, and D. L. Feldheim, Advanced Materials **11**, 447 (1999).

[30] C. S. Barton *et al.*, Functional monolayer surfaces on gold nanoparticles for specific binding of histidine-tagged proteins, in *Nanoscience and Nanotechnology, 2006. ICONN '06. International Conference on*, 2006.

[31] P. D. Jadzinsky, G. Calero, C. J. Ackerson, D. A. Bushnell, and R. D. Kornberg, Science **318**, 430 (2007).

[32] M. Brust, M. Walker, D. Bethell, D. J. Schiffrin, and R. Whyman, Journal of the Chemical Society , 801 (1994).

[33] N. Lala, S. P. Lalbegi, S. D. Adyanthaya, and M. Sastry, Langmuir **17**, 3766 (2001).

[34] M. Sastry, A. Kumar, and P. Mukherjee, Colloids and Surfaces A: Physicochemical and Engineering Aspects **181**, 255 (2001).

[35] B. Xu and N. J. Tao, Science **301**, 1221 (2003).

[36] R. Voggu, P. Suguna, S. Chandrasekaran, and C. N. R. Rao, Chemical Physics Letters **443**, 118 (2007).

[37] J. P. Collman *et al.*, Science **315**, 1565 (2007).

[38] X. Zou *et al.*, Journal of Colloid and Interface Science **295**, 401 (2006).

[39] K. Keren, R. S. Berman, E. Buchstab, U. Sivan, and E. Braun, Science **302**, 1380 (2003).